

Multiple scale approach to estimation of scintillator characteristics



Andrey N. Vasil'ev^a, Alexandr Gektin^b
^aSkobeltsyn Institute of Nuclear Physics, Lomonosov
Moscow State University, Moscow, Russia

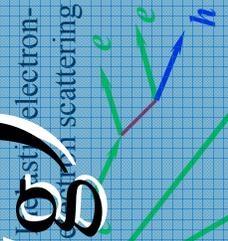
^b*Institute for Scintillation Materials, Kharkiv, Ukraine*



Cascade

-1

(βE_g)



Transport

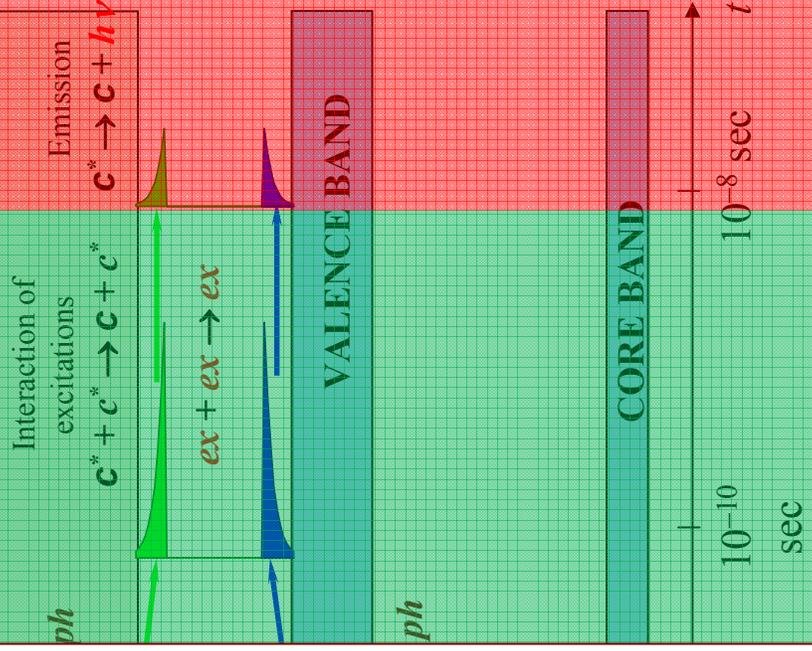
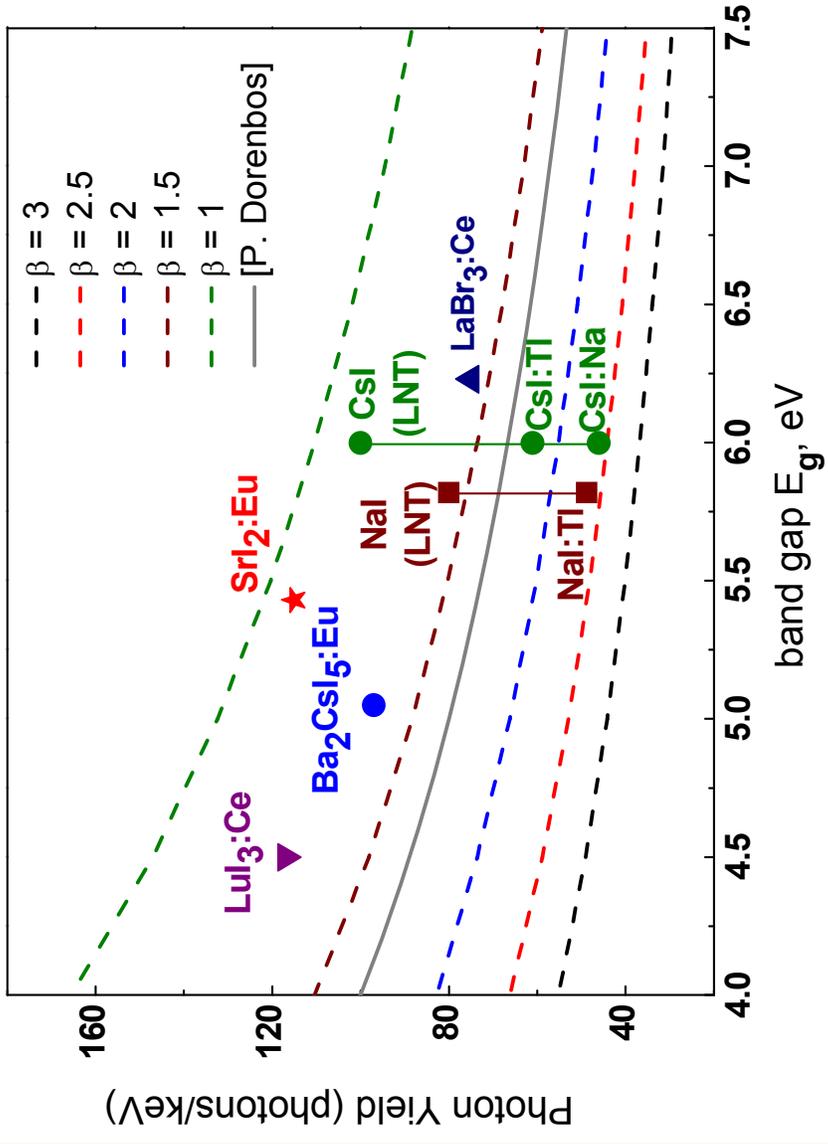
S

Thermalization of electrons and holes by different processes
Creation of excitons, capture of electrons and holes by different

Center

Q

CONDUCTION BAND



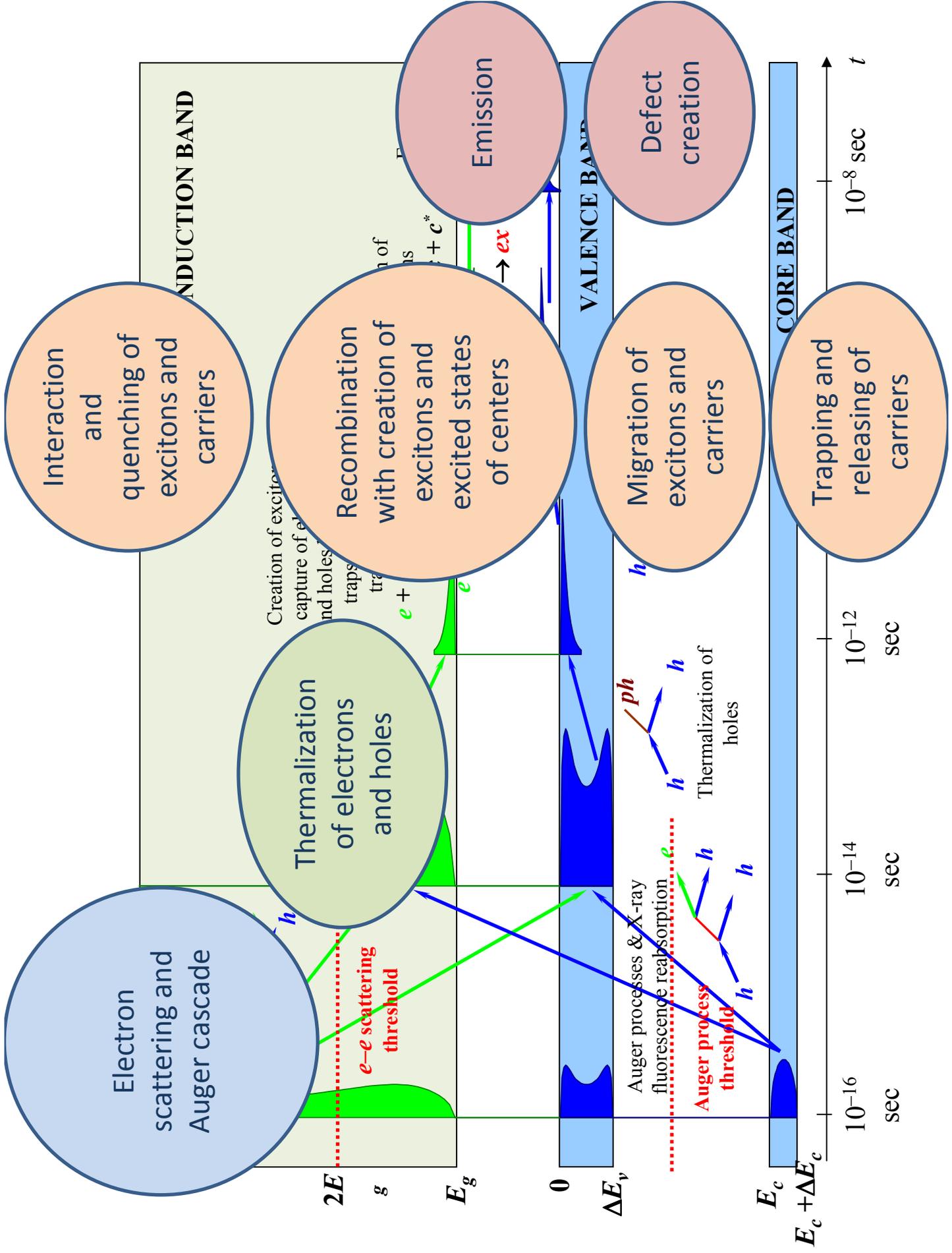
Applications and material engineering request
quantitative predictions of properties of new
scintillating materials

Simple estimation of scintillation efficiency as β SQ
(cascade-transport-center) is only qualitative

~~New theory of scintillations?~~

Re-estimation of the role of different stages of energy
relaxation in crystals on the basis of deeper
experimental investigation of new materials

Contemporary model: Scintillation as collective
interconnected processes of spatial and temporal
evolution of strongly non-equilibrium excited region in
media



Electron scattering and Auger cascade

Thermalization of electrons and holes

Interaction and quenching of excitons and carriers

Recombination with creation of excited states of centers

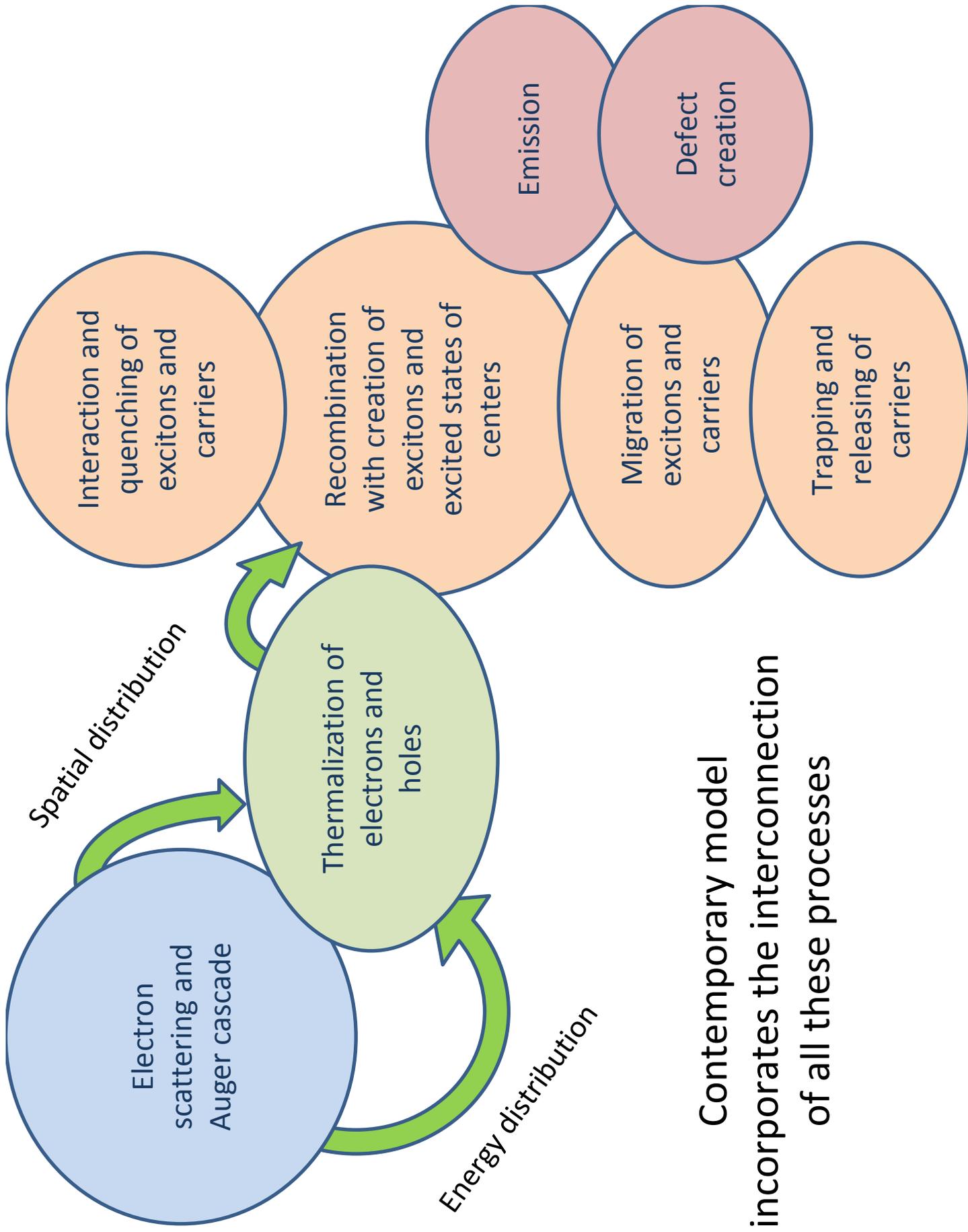
Emission

Defect creation

Migration of excitons and carriers

Trapping and releasing of carriers

Are these processes independent?
NO!

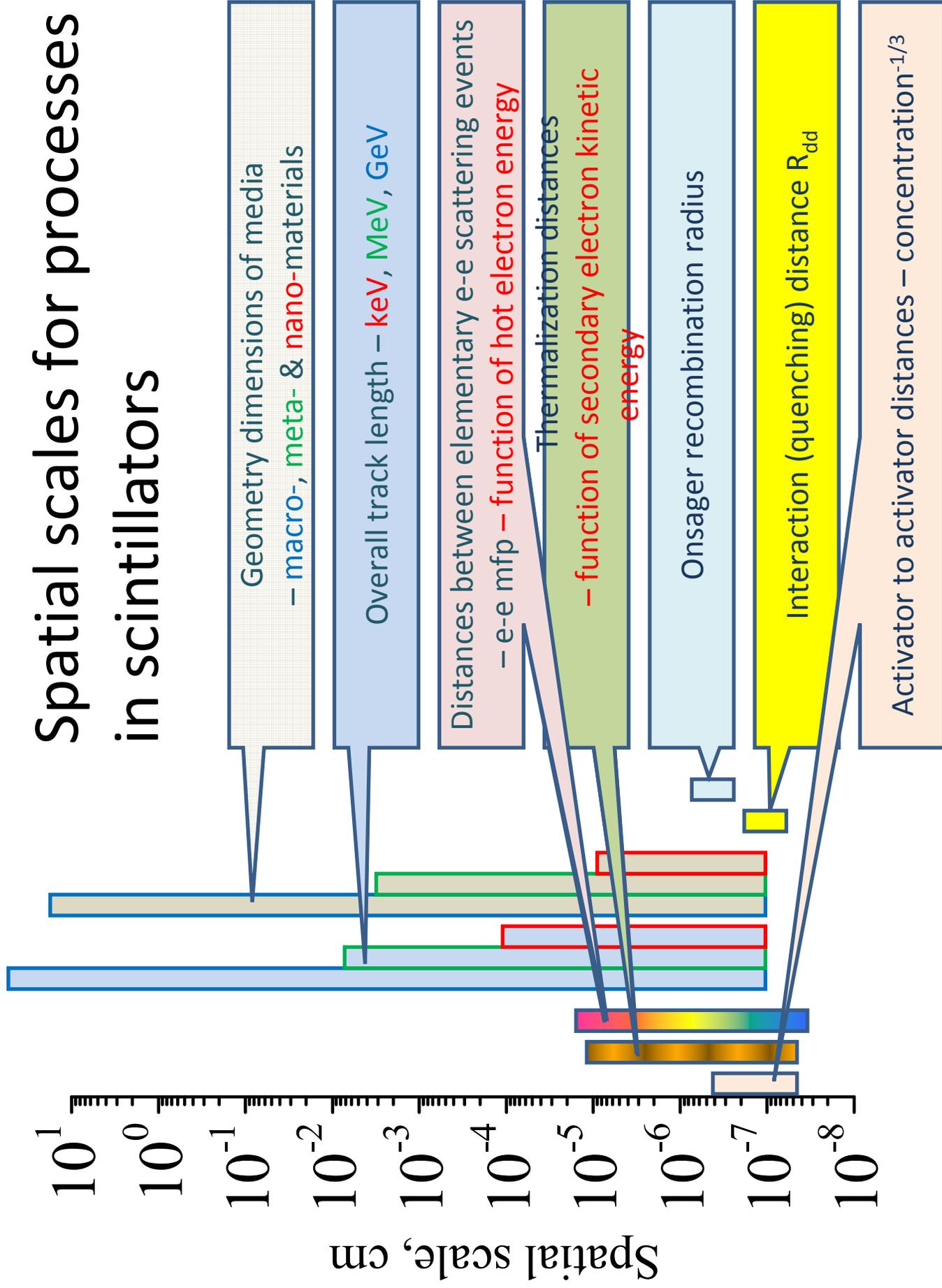


Contemporary model
incorporates the interconnection
of all these processes

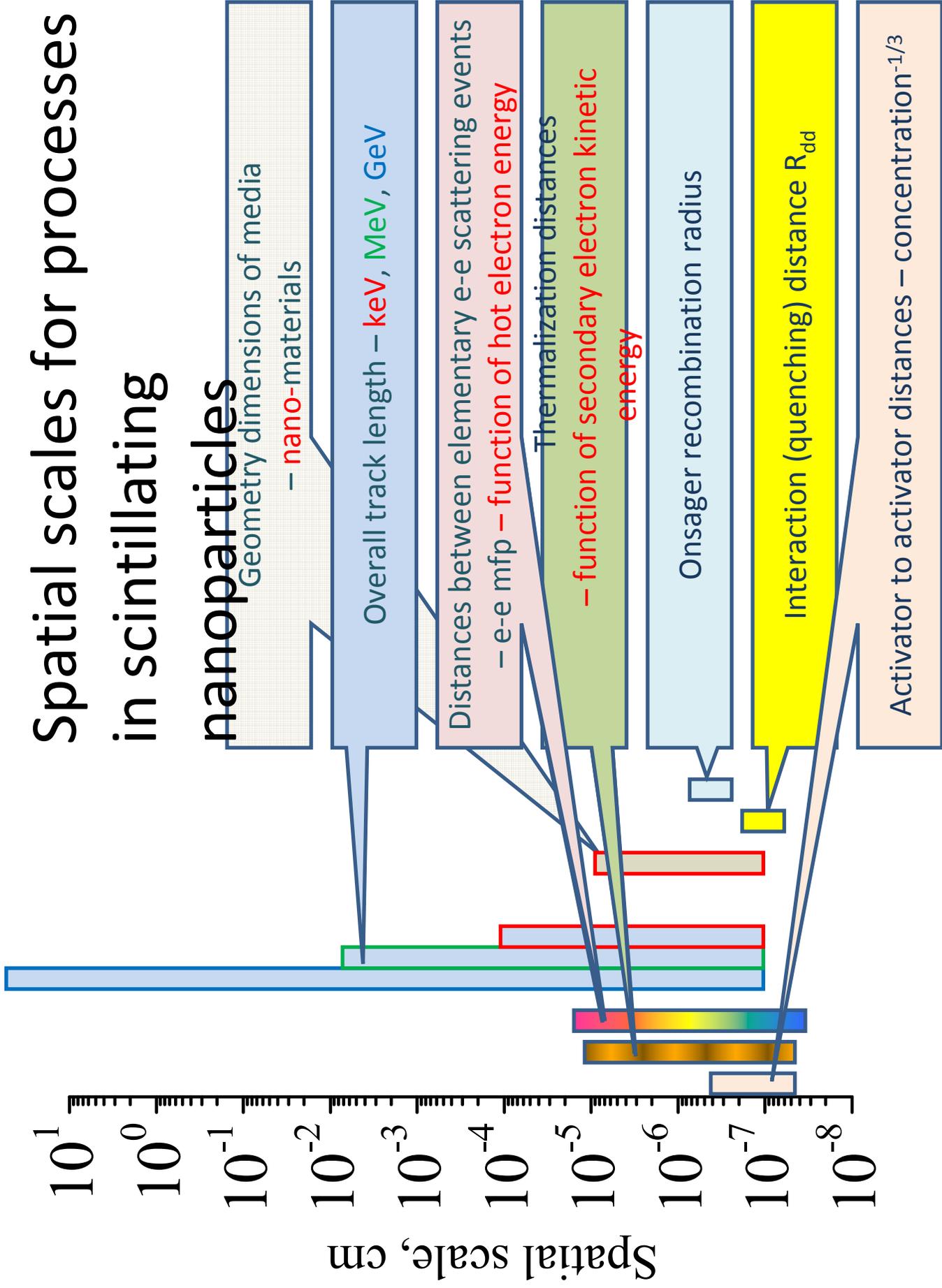
Outline

- Spatial scales for processes in scintillators
- Nanoparticles as scintillators
- Cascade, thermalization and recombination
- Different types of mobilities
- Thermalization length for different types of crystals
- Interconnection of cascade, thermalization and recombination stages in binary iodides
- Why cascade is so effective in CsI?
- Thermalization length and impurities
- Concluding remarks

Spatial scales for processes in scintillators

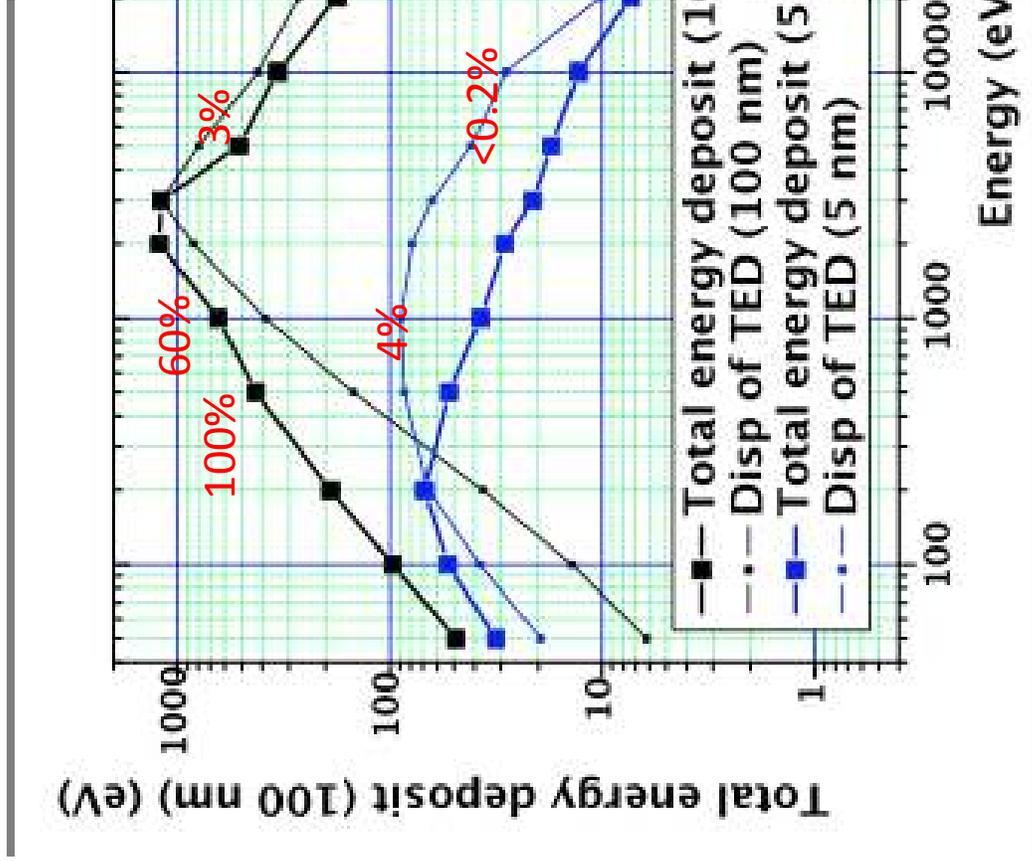


Spatial scales for processes in scintillating nanoparticles



Energy deposited within nanoparticles

Total energy deposited as a function of the energy of the primary electron



Vistovskyy *et al.* J. Appl. Phys. 112, 024325 (2012)

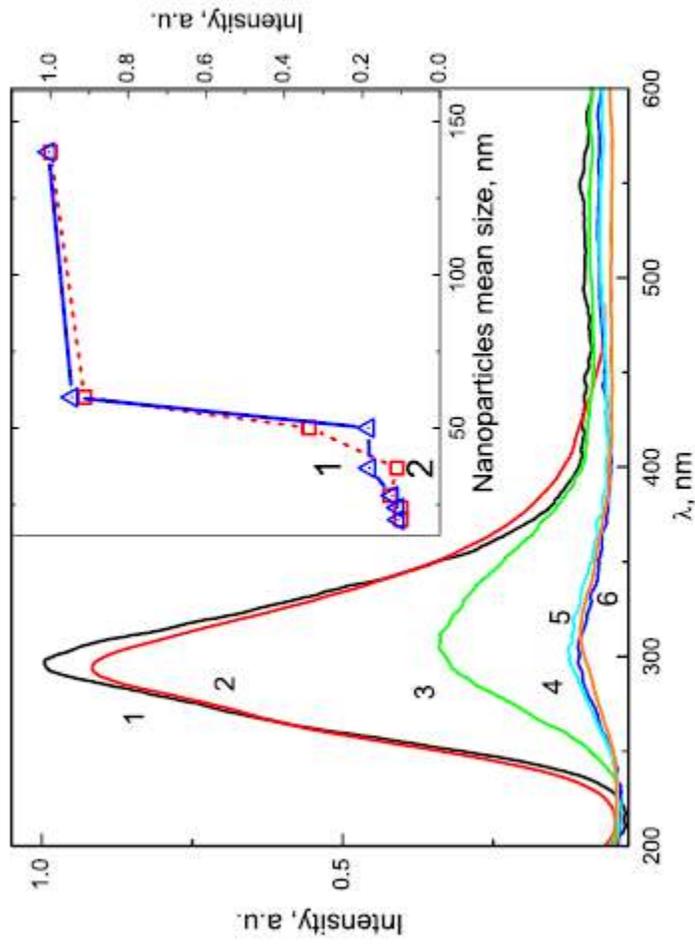
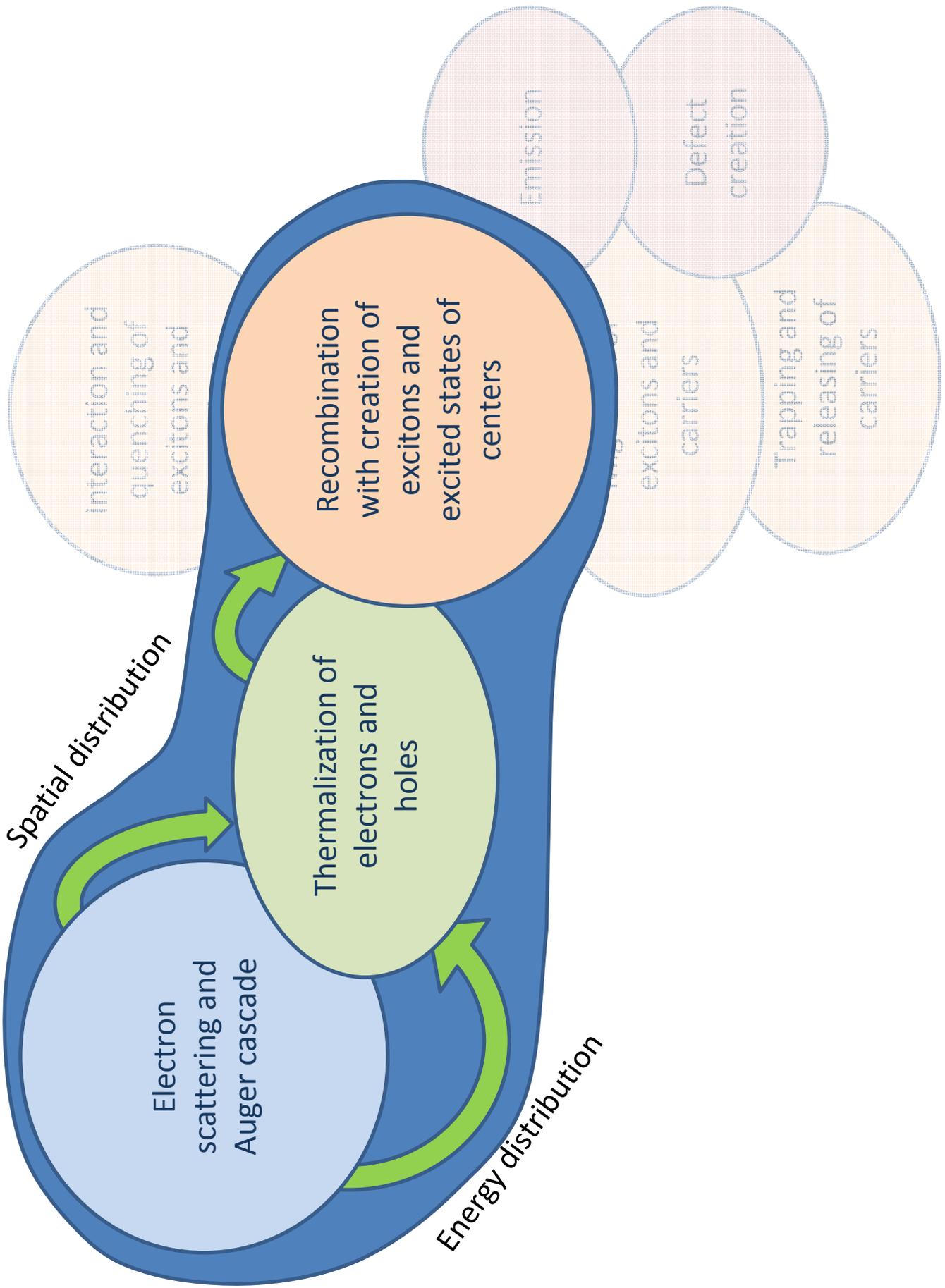
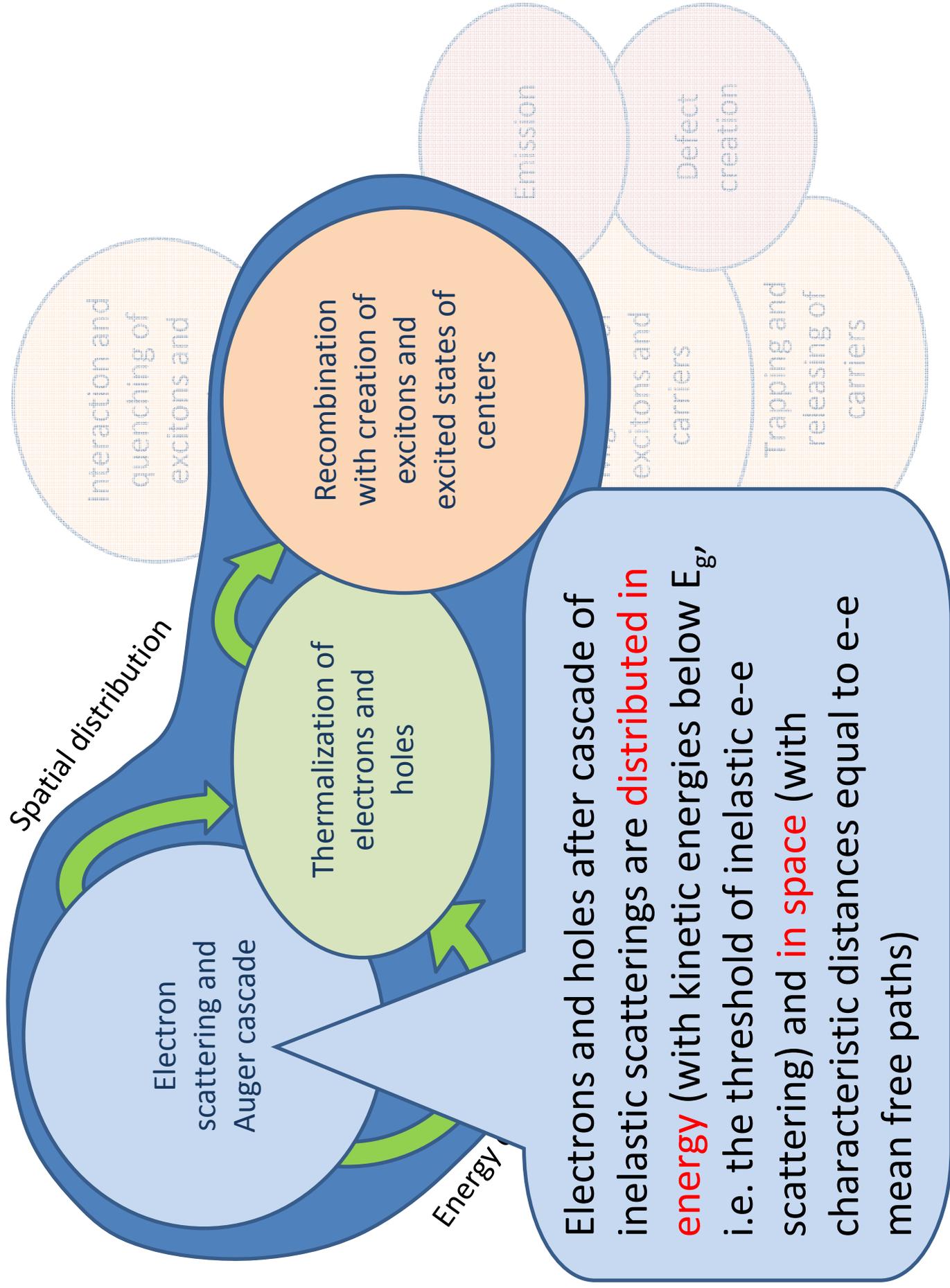


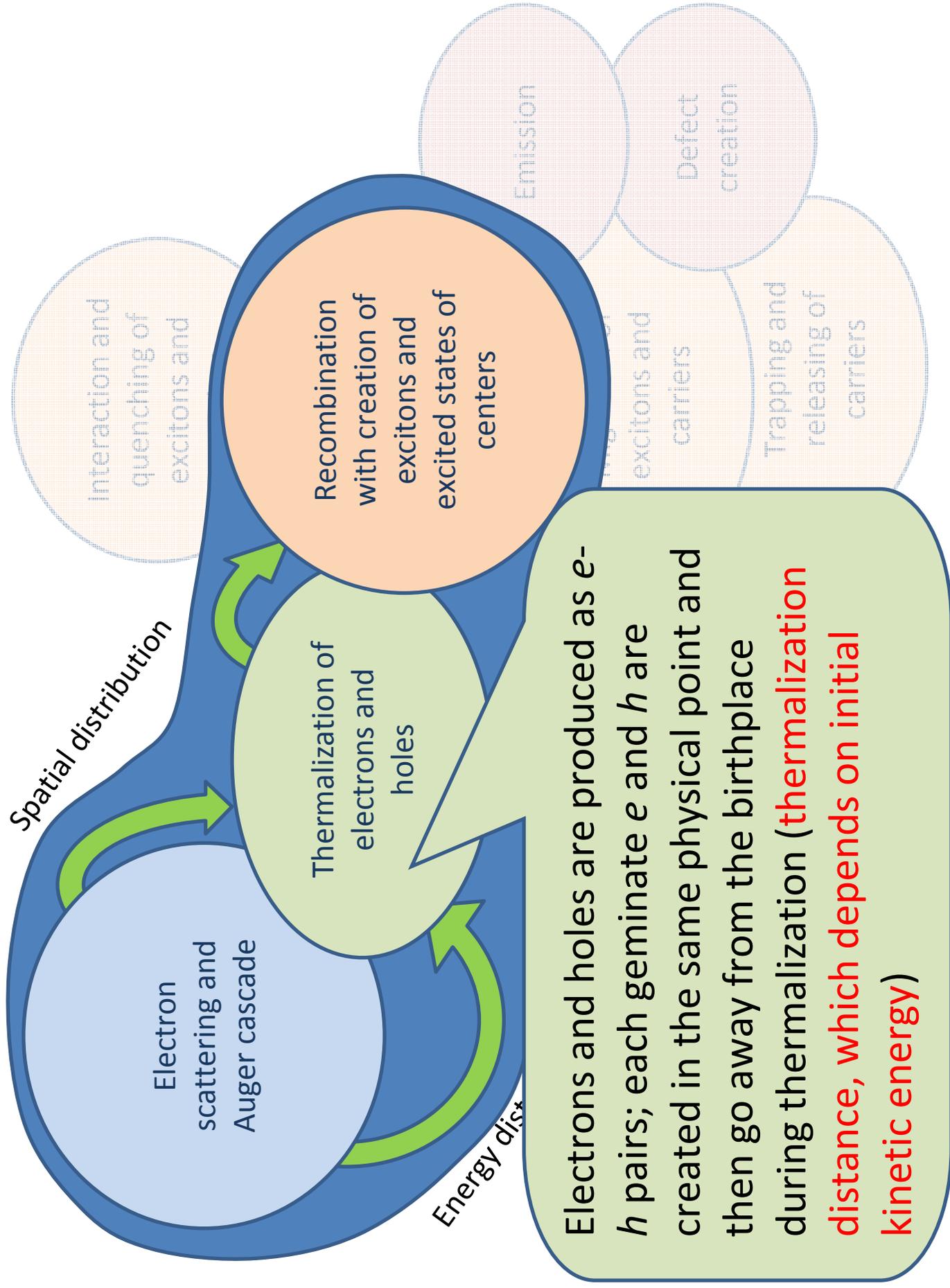
FIG. 6. X-ray excited luminescence spectra of CaF_2 nanoparticles of various size at 300 K. Curves: 1–140; 2–60; 3–50; 4–37; 5–28; 6–20 nm. The dependence of normalized luminescence intensity on the nanoparticle size is shown on inset: curve 1—luminescence intensity upon the excitation by quanta with energy $h\nu_{\text{exc}} = 16 \text{ eV}$, curve 2—X-ray excited luminescence intensity.

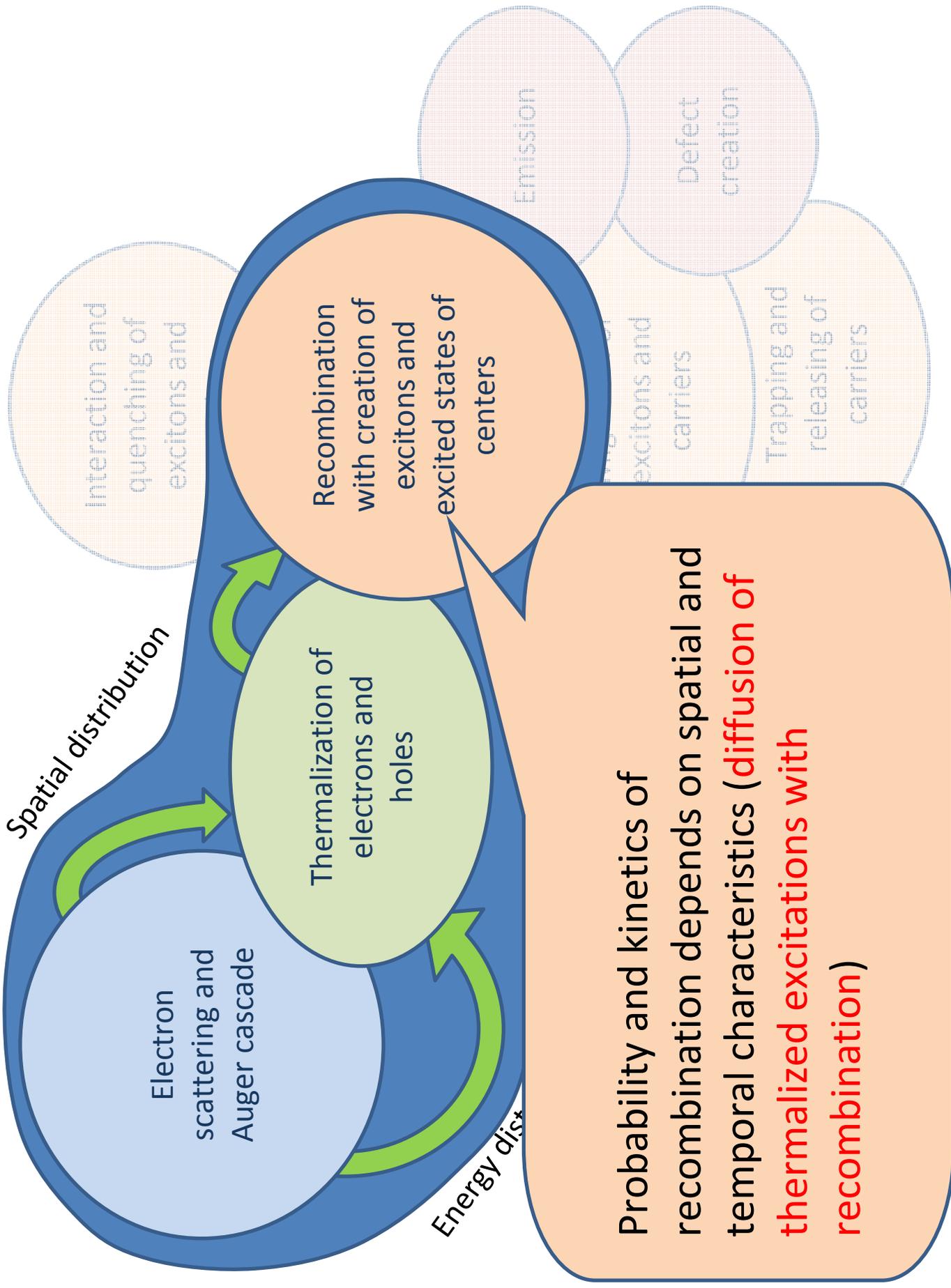
Outline

- Spatial scales for processes in scintillators
- Nanoparticles as scintillators
- **Cascade, thermalization and recombination**
- Different types of mobilities
- Thermalization length for different types of crystals
- Interconnection of cascade, thermalization and recombination stages in binary iodides
- Why cascade is so effective in CsI?
- Thermalization length and impurities
- Concluding remarks







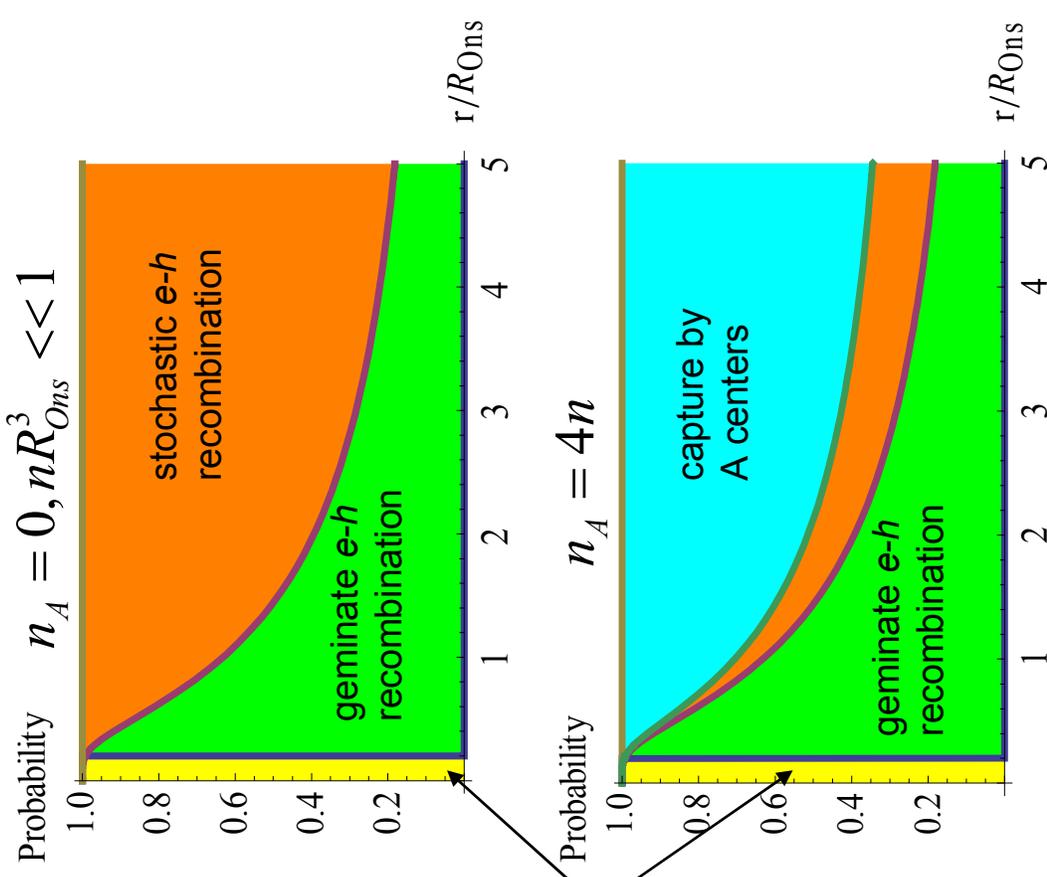


Probability and kinetics of recombination depends on spatial and temporal characteristics (**diffusion of thermalized excitations with recombination**)

Onsager model without screening

$$U(r) = -\frac{e^2}{4\pi\epsilon_0\epsilon r}$$

$$U(R_c) = -k_B T \Rightarrow R_c = R_{Ons} \equiv \frac{e^2}{4\pi\epsilon_0\epsilon k_B T}$$



In the presence of centers A some part of escaped electrons are captured by centers (tarps)

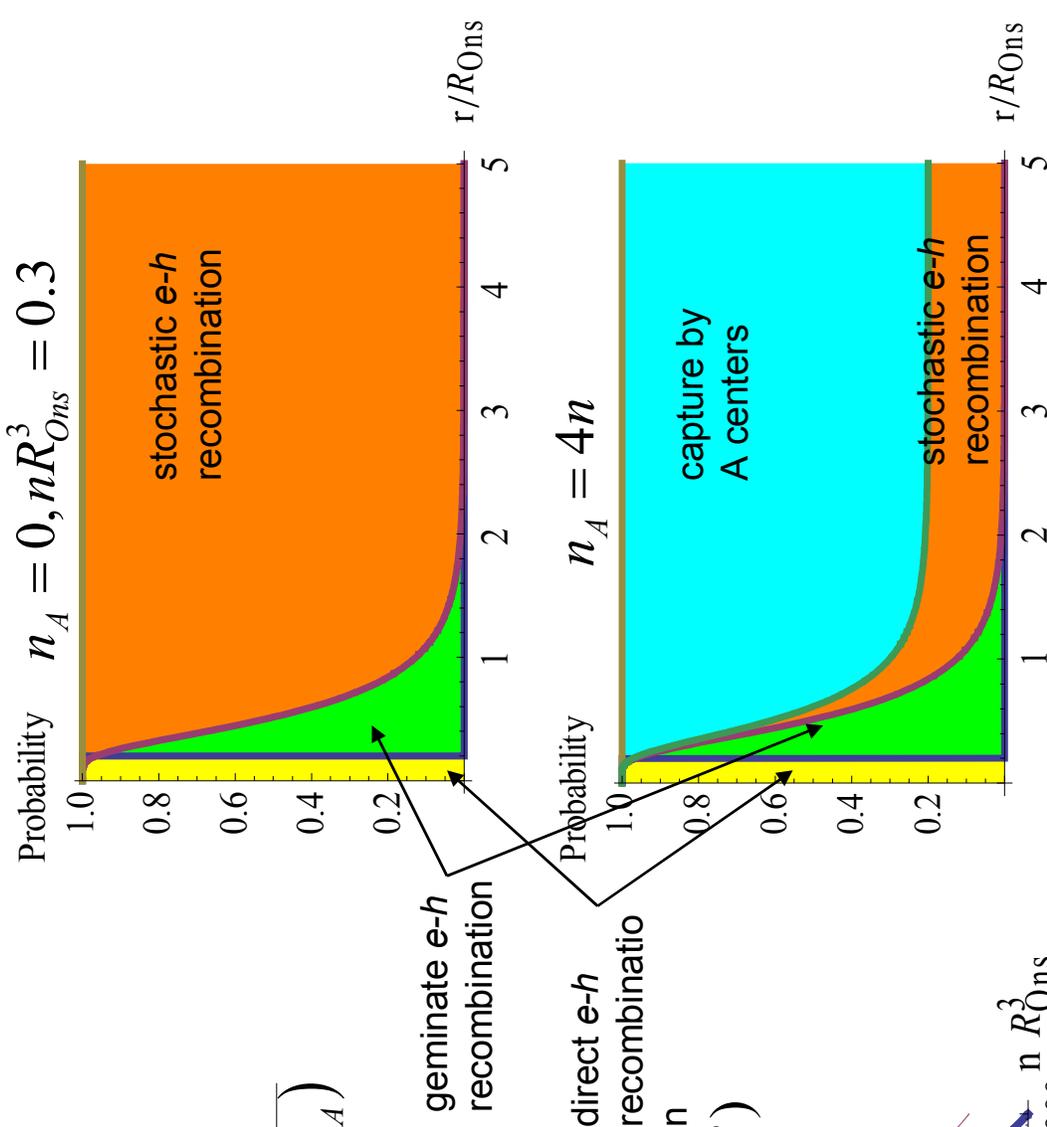
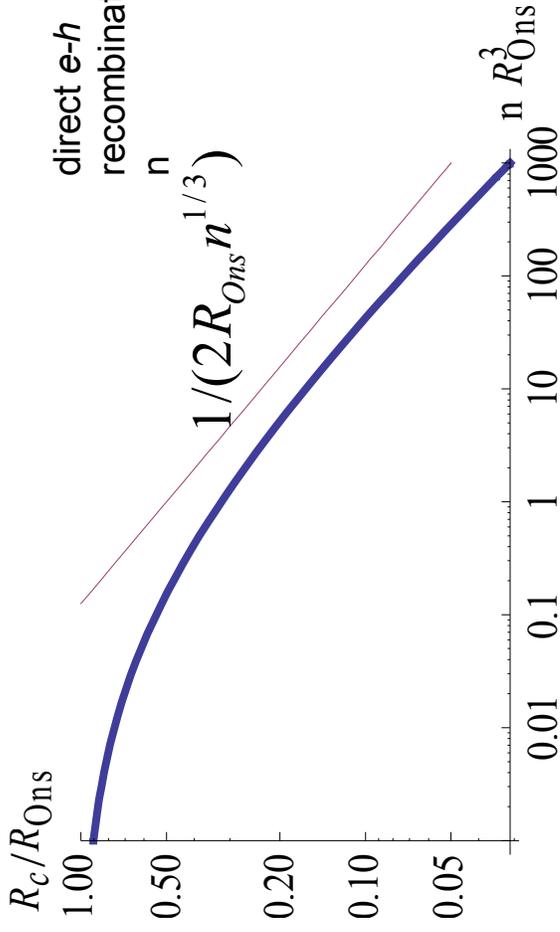
Onsager model with account for screening

$$U(r) = -\frac{e^2}{4\pi\epsilon_0\epsilon r} \exp\left(-\frac{r}{\lambda_D}\right)$$

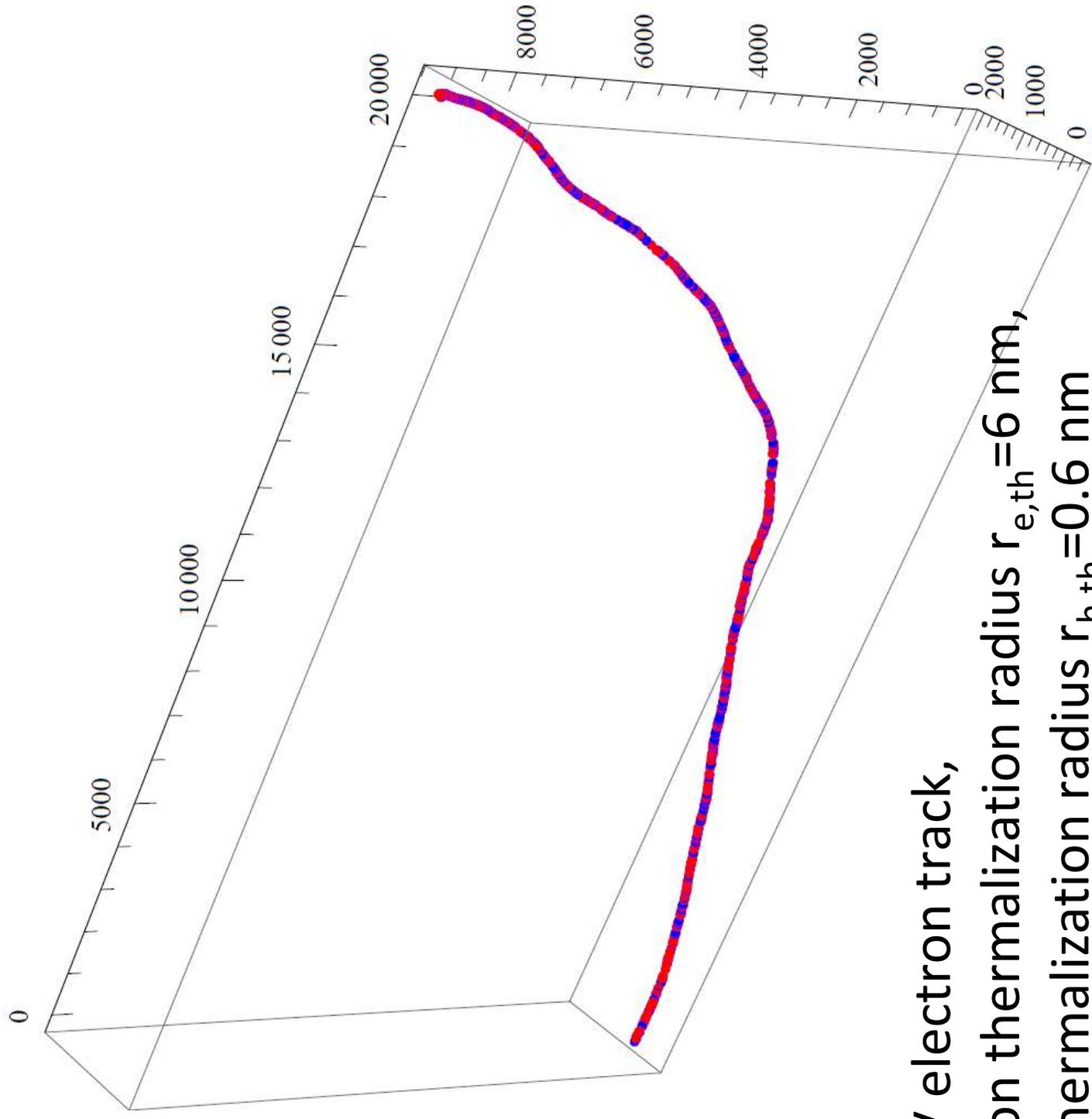
Debye screening constant

$$\frac{1}{\lambda_D} \equiv \sqrt{\frac{e^2(n+n_A)}{\epsilon_0\epsilon k_B T}} = \sqrt{4\pi R_{Ons}(n+n_A)}$$

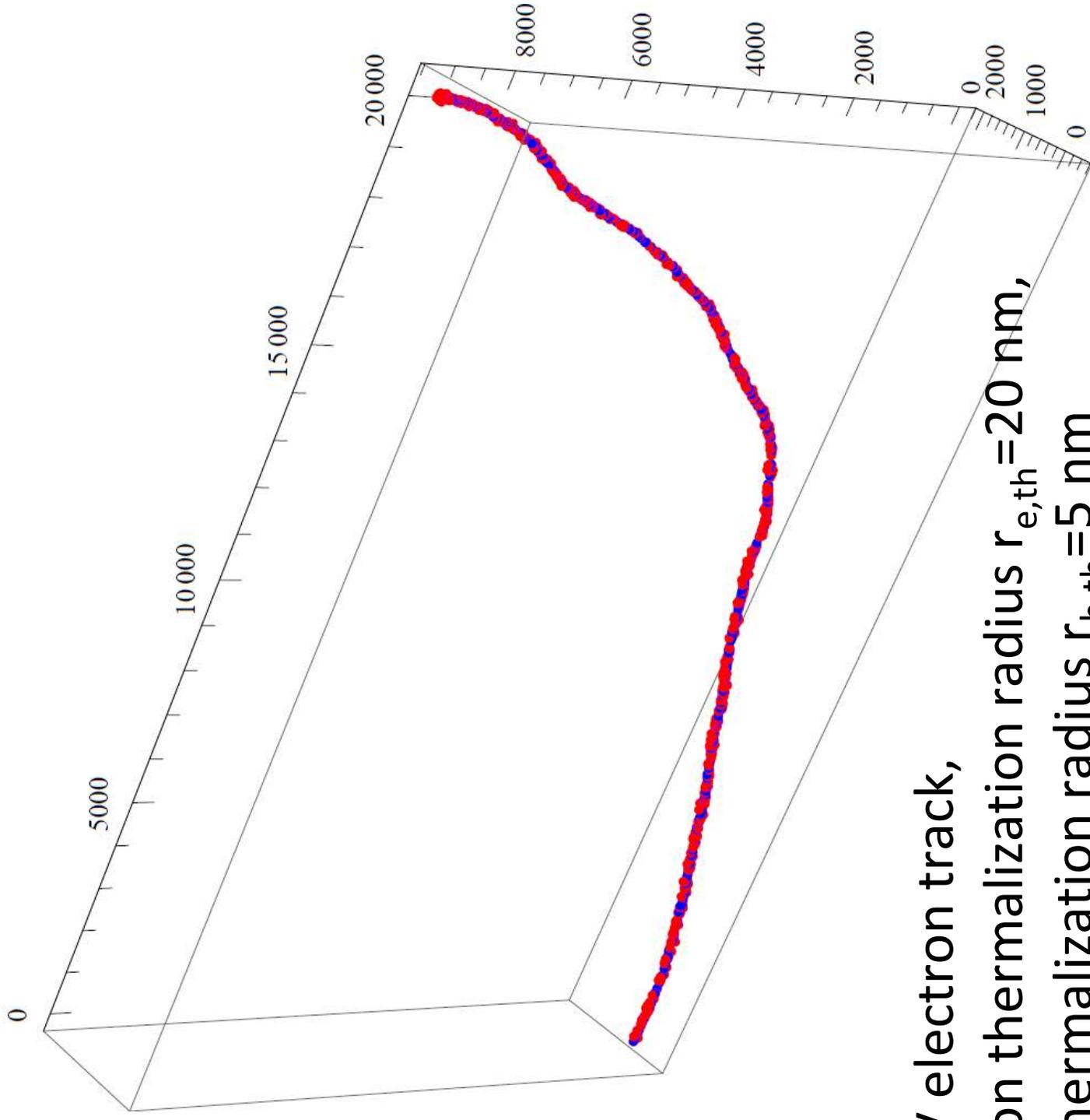
$$U(R_c) = -k_B T$$



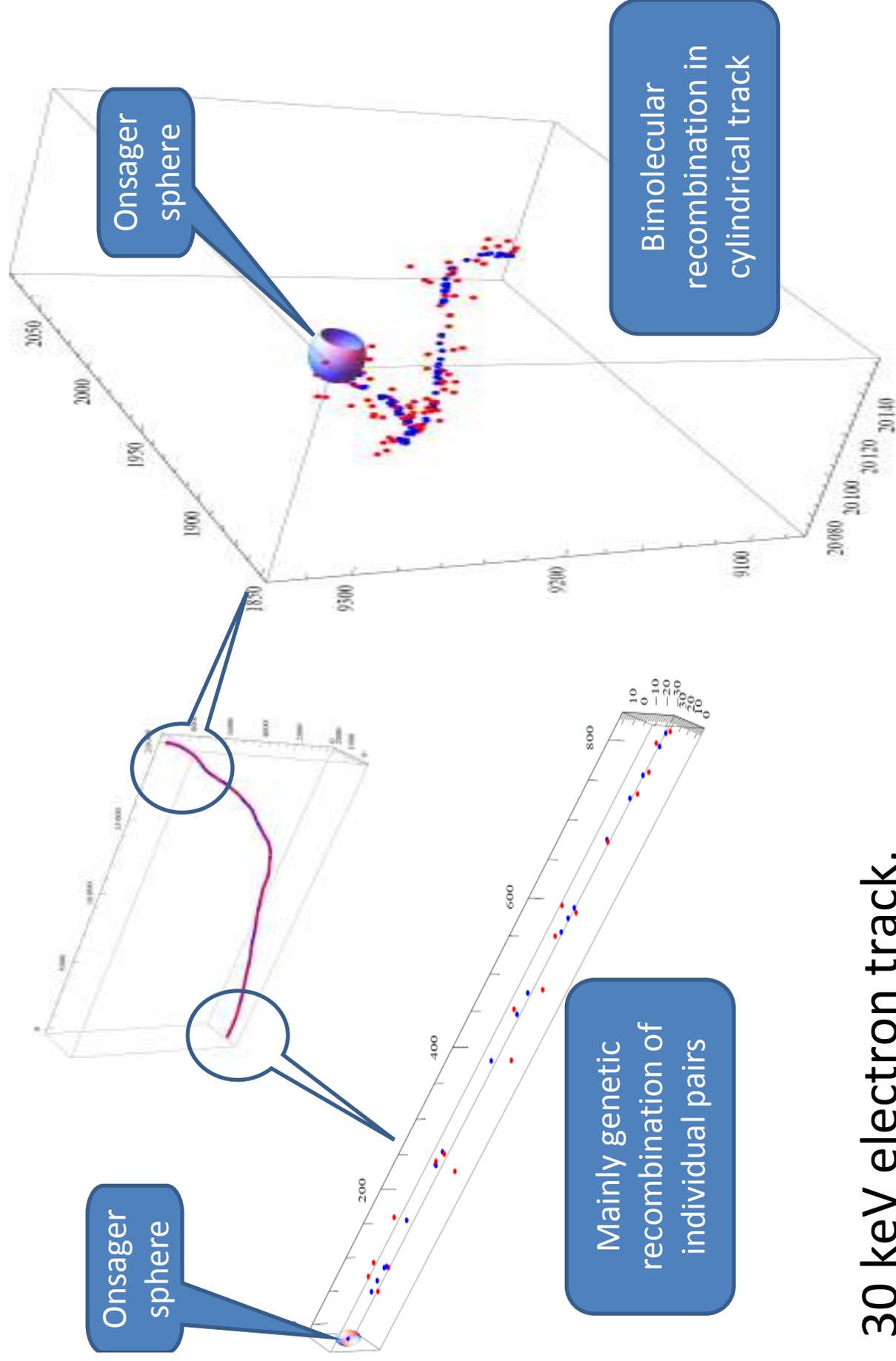
Example of structure of excited
region after 30 keV electron
passage



30 keV electron track,
electron thermalization radius $r_{e,th}=6$ nm,
hole thermalization radius $r_{h,th}=0.6$ nm



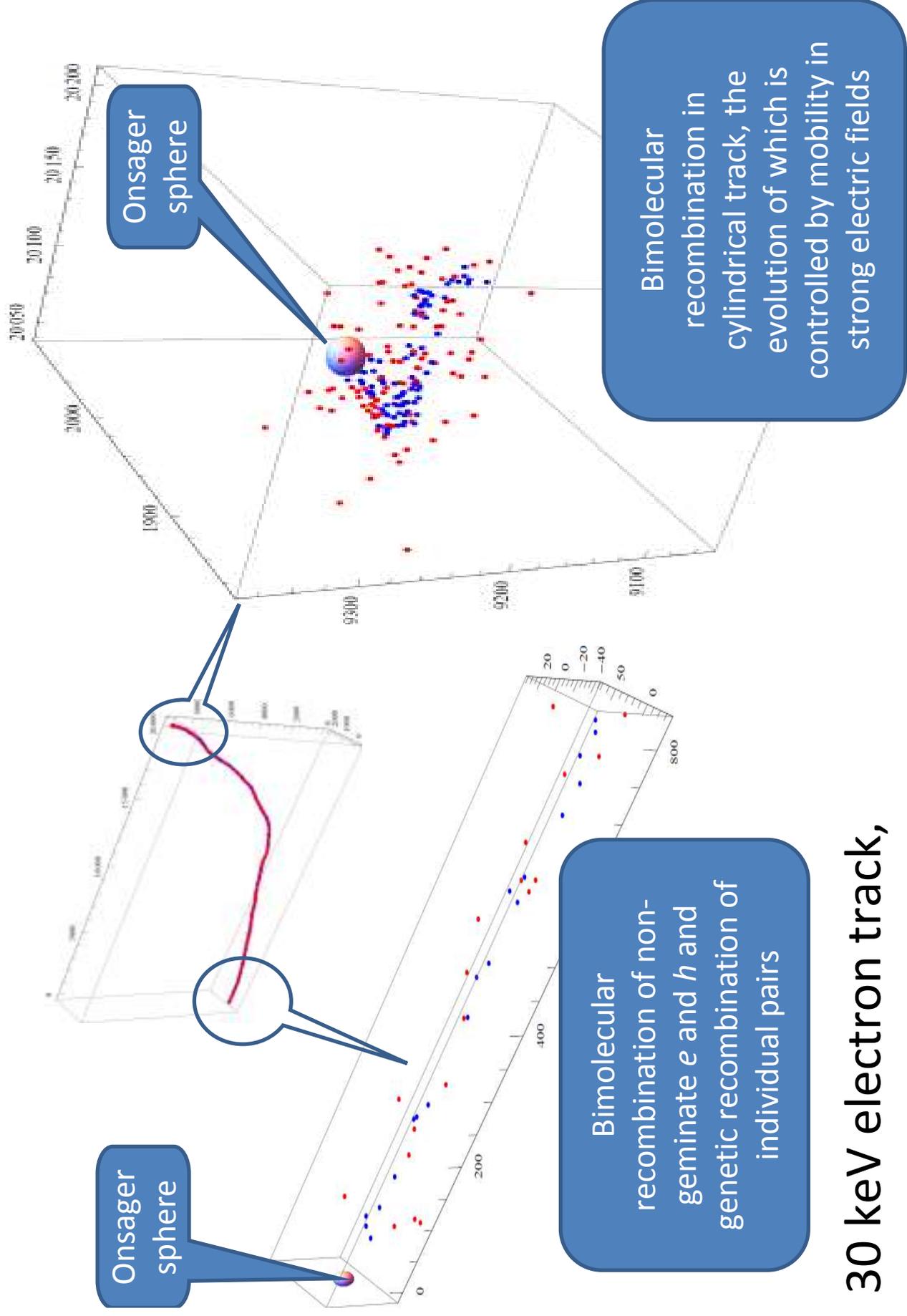
30 keV electron track,
electron thermalization radius $r_{e,th}=20$ nm,
hole thermalization radius $r_{h,th}=5$ nm



30 keV electron track,

$r_{e,th} = 6 \text{ nm}$,

$r_{h,th} = 0.6 \text{ nm}$ (red=e, blue=h)



Onsager sphere

Bimolecular recombination of non-geminate e and h and genetic recombination of individual pairs

Bimolecular recombination in cylindrical track, the evolution of which is controlled by mobility in strong electric fields

30 keV electron track,

$r_{e,th} = 20 \text{ nm}$,

$r_{h,th} = 5 \text{ nm}$ (red= e , blue= h)

Outline

- Spatial scales for processes in scintillators
- Nanoparticles as scintillators
- Cascade, thermalization and recombination
- **Different types of mobilities**
- Thermalization length for different types of crystals
- Interconnection of cascade, thermalization and recombination stages in binary iodides
- Why cascade is so effective in CsI?
- Thermalization length and impurities
- Concluding remarks

Non-proportionality and mobility

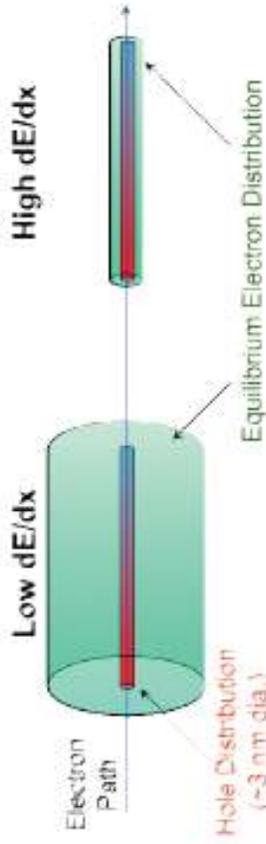


Figure 4. Difference between equilibrium diameters of the electrons (assuming immobile holes) for two different ionizations. Low density is on the left, high density is on the right.

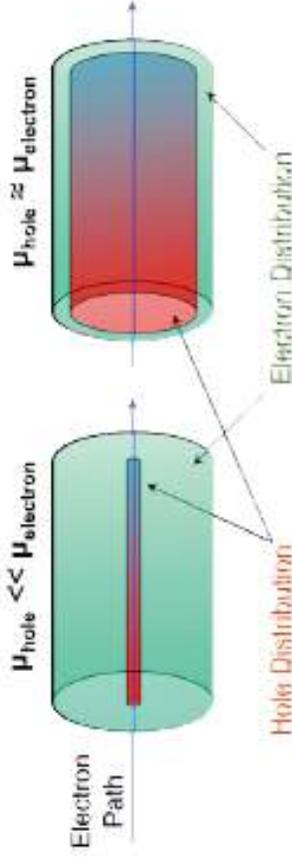


Figure 5. Relative sizes of electron and hole diameters as a function of relative hole mobility. The left side illustrates the distributions when the electron mobility is significantly higher than then hole mobility, while the right side illustrates the distributions when they have similar mobilities.

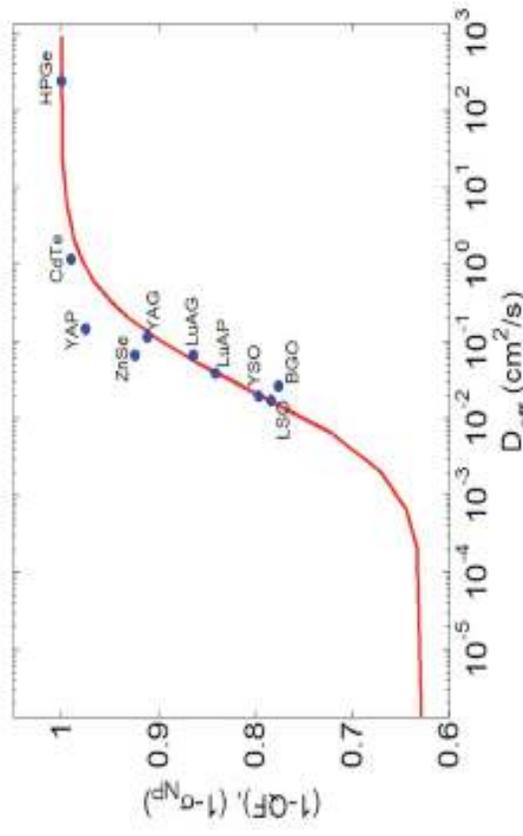


Figure 6. Measured relative light yield at low electron energy for a number of scintillators (solid points) and predicted luminescence (solid curve) as a function of diffusion coefficient. Reprinted with permission from [61]. See text for definitions.

W. W. Moses, G. A. Bizarri, R. T. Williams, S. A. Payne, A. N. Vasil'ev, J. Singh, Q. Li, J. Q. Grim, and W-S. Choong, *The Origins of Scintillator Non-Proportionality*, IEEE Transactions on Nuclear Science, vol. 59, issue 5, pp. 2038-2044 (2012)

Spatial distribution of electrons, holes and excitons

due to mobility in e-e passive energy domain

- Two types of carrier mobilities: **thermalization length (mobility of hot electrons and holes)** and **mobility of thermalized excitations (electrons, holes & excitons)**.
- High-energy part of ionization track – individual electron-hole pairs and small non-overlapping clusters of excitations. **Negative role of mobility**: the higher the **thermalization length** (in comparison with Onsager radius), the lower the recombination yield (HPGe – the limiting case of high mobility w/o any luminescence).
- Low-energy part of ionization track – overlapping clusters of excitations. Mean distance between interacting excitations increases with increase of the mobility of excitons. **Positive role of mobility**: the higher the mobility, the lower the quenching of excitation due to high EE density.
- “Ideal” scintillator: **Low hot mobility (high yield of excitons)** and **high thermalized mobility (low interaction)**.

Outline

- Spatial scales for processes in scintillators
- Nanoparticles as scintillators
- Cascade, thermalization and recombination
- Different types of mobilities
- **Thermalization length for different types of crystals**
- Interconnection of cascade, thermalization and recombination stages in binary iodides
- Why cascade is so effective in CsI?
- Thermalization length and impurities
- Concluding remarks

Coupled processes of thermalization and spatial diffusion

Four main functions which characterized spatial diffusion and thermalization:

(1) rate of electron-phonon scattering (inverse lifetime) $\tau^{-1}(E_e^{kin})$

(2) mean free path $\lambda(E_e^{kin}) = v(E_e^{kin})\tau(E_e^{kin})$

(3) spatial diffusion coefficient $D^R(E_e^{kin}) = \frac{1}{3}v^2(E_e^{kin})\tau(E_e^{kin})$ and
equation for Brownian motion

$$\frac{d \langle r^2 \rangle}{dt} = 6D^R(E_e^{kin})$$

(4) energy relaxation rate $S(E_e^{kin}) = D^E(E_e^{kin})/k_B T$ and
energy relaxation equation

$$\frac{dE_e^{kin}}{dt} = -S(E_e^{kin})$$

$$\frac{d \langle r^2 \rangle}{dE_e^{kin}} = -6 \frac{D^R(E_e^{kin})}{S(E_e^{kin})}$$

Coupled processes of thermalization and spatial diffusion

Mean square of the thermalization distance $\langle r^2 \rangle_{E_{e0} \rightarrow E_e^{kin}} = 6 \int_{E_e^{kin}}^{E_{e0}} \frac{D^R(E')}{S(E')} dE'$

Spatial distribution function $f(r, l_e(E_{e0})) = \frac{3\sqrt{6} r^2}{\sqrt{\pi} l_e^3(E_{e0})} \exp\left(-\frac{3r^2}{2l_e^2(E_{e0})}\right)$

where thermalization length is $l_e(E_{e0}) = \sqrt{\langle r^2 \rangle_{E_{e0} \rightarrow k_B T}}$

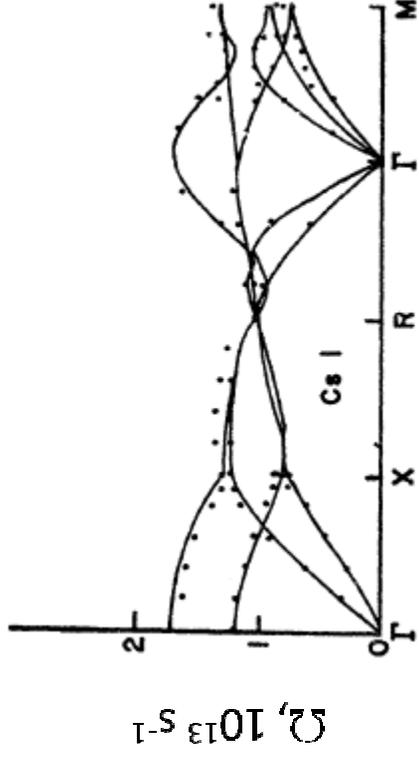
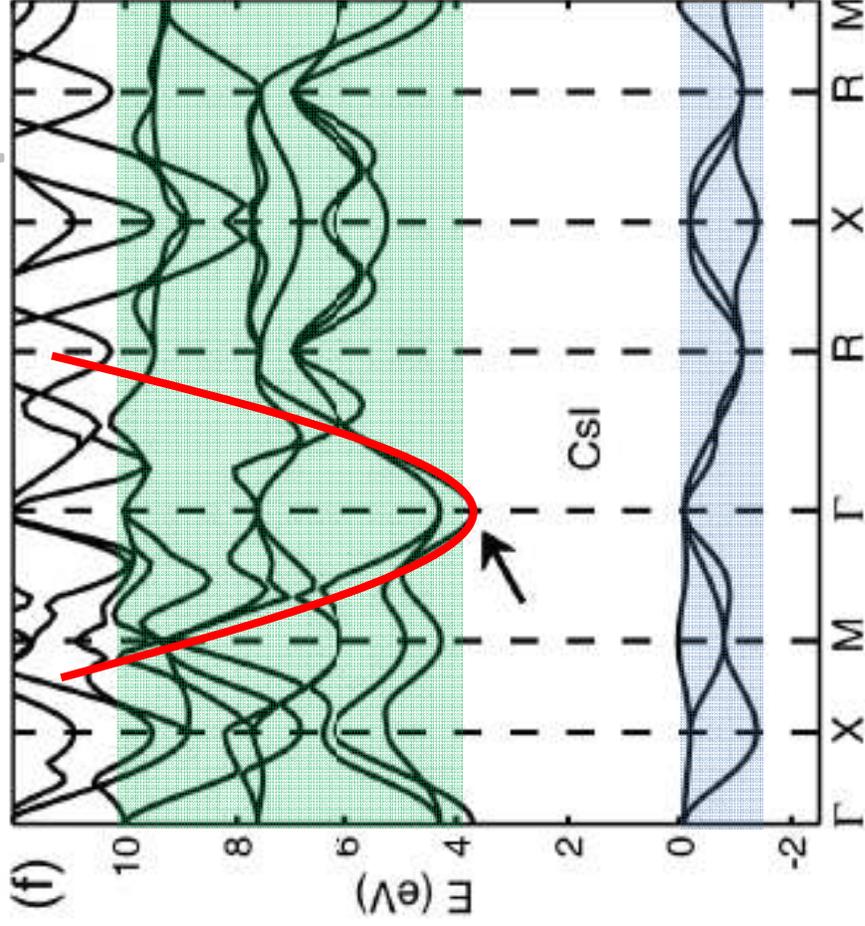
Thermalization length for one LO phonon branch

$$l_{e,LO}^2(E_{e0}) = \frac{8}{3} a_B^2 \left(\frac{\tilde{\xi}}{m_e^*/m_0} \right)^2 \tanh\left(\frac{\hbar\Omega_{LO}}{2k_B T}\right)_{\hbar\Omega_{LO}}^{E_{e0}} \int \left(\frac{E'}{\hbar\Omega_{LO}}\right)^2 \frac{1}{\ln(4E'/\hbar\Omega_{LO})} \hbar\Omega_{LO} dE'$$

$$= \frac{1}{24} a_B^2 \left(\frac{\tilde{\xi}}{m_e^*/m_0} \right)^2 \tanh\left(\frac{\hbar\Omega_{LO}}{2k_B T}\right) \text{Ei}\left(3 \ln\left(\frac{4E_{e0}}{\hbar\Omega_{LO}}\right)\right),$$

CsI band structure and phonon dispersion

dispersion



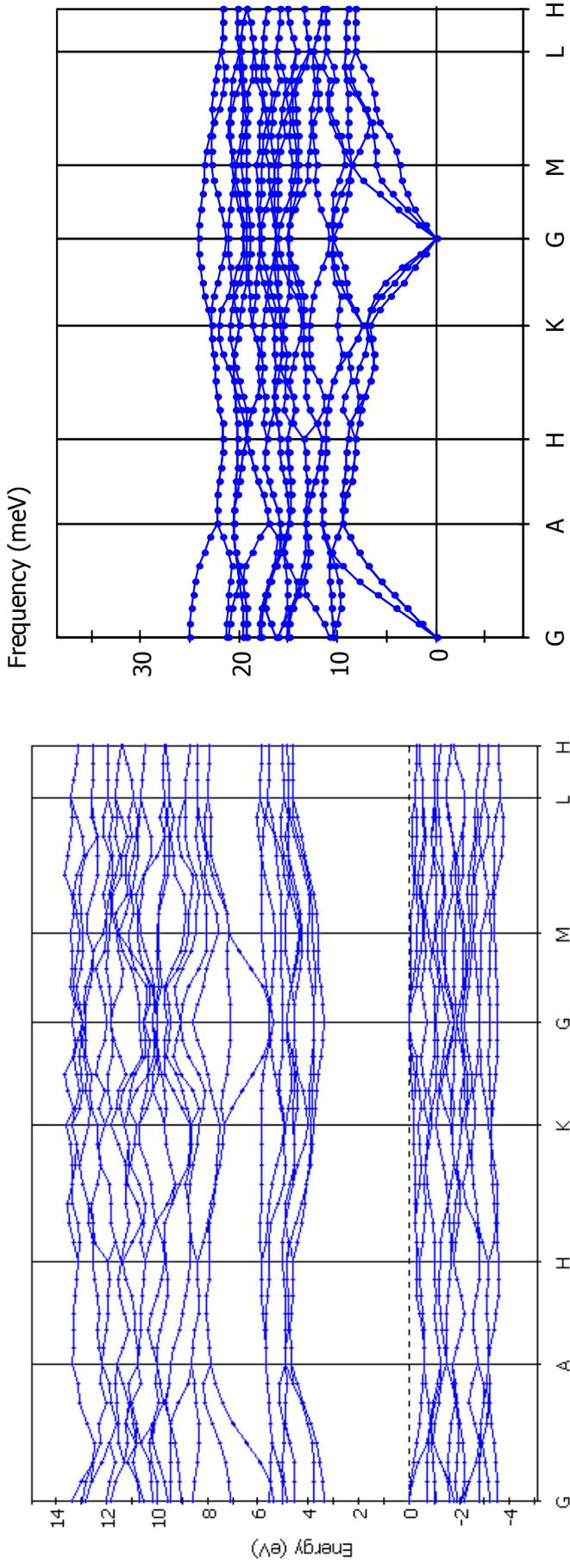
J.F. Vetelino, K. V. Namjoshi and S. S. Mitra,
 Phys. Rev. B 7, 4001-4004 (1973)

Band structure calculations

from W. Setyawan, R. M. Gaume et al. *IEEE TNS*, 2009

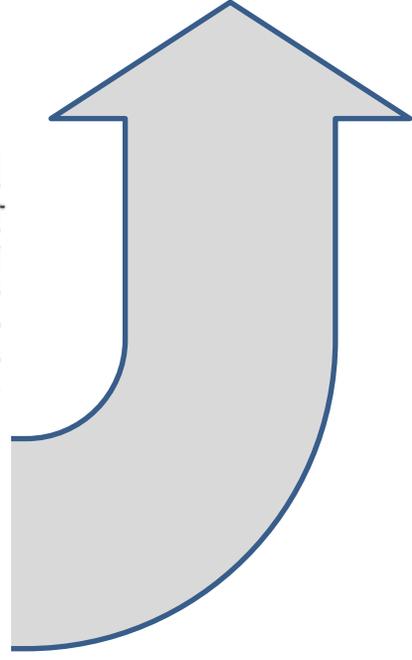
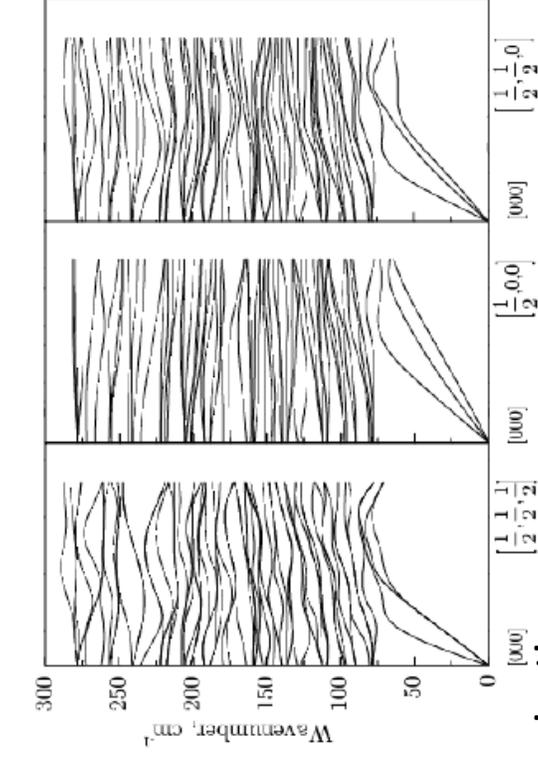
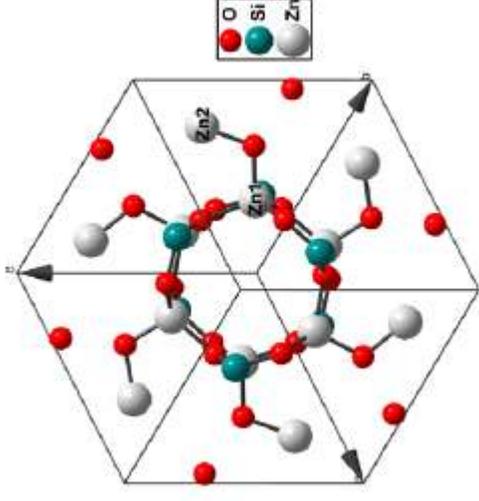
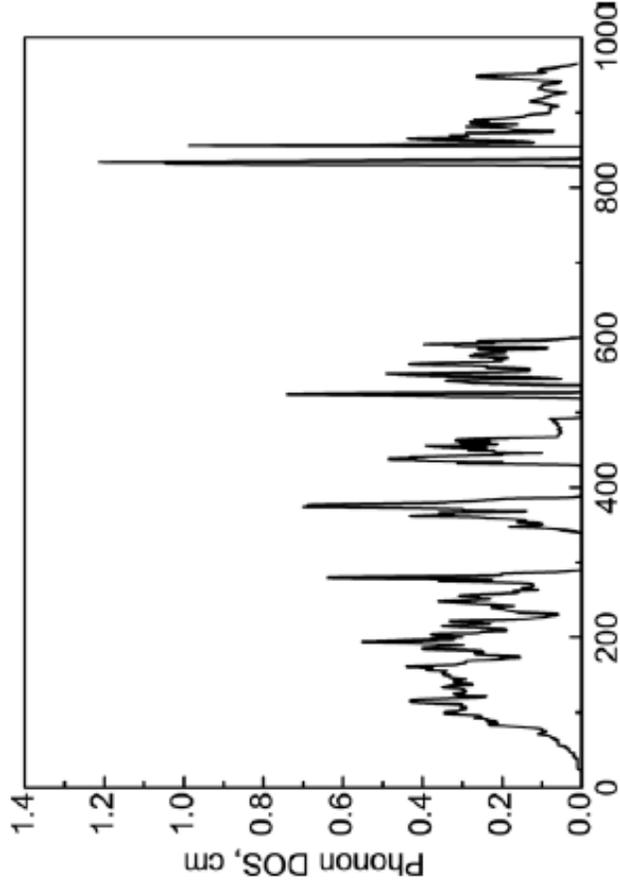
LaBr₃ band structure (w/o La4f) and phonon dispersion

I. Iskandarova, private communication



Band structure for LaBr₃ (without La f states). Energy scale is shifted to the top of the valence band.

Zn₂SiO₄ (42 atoms per unit cell)

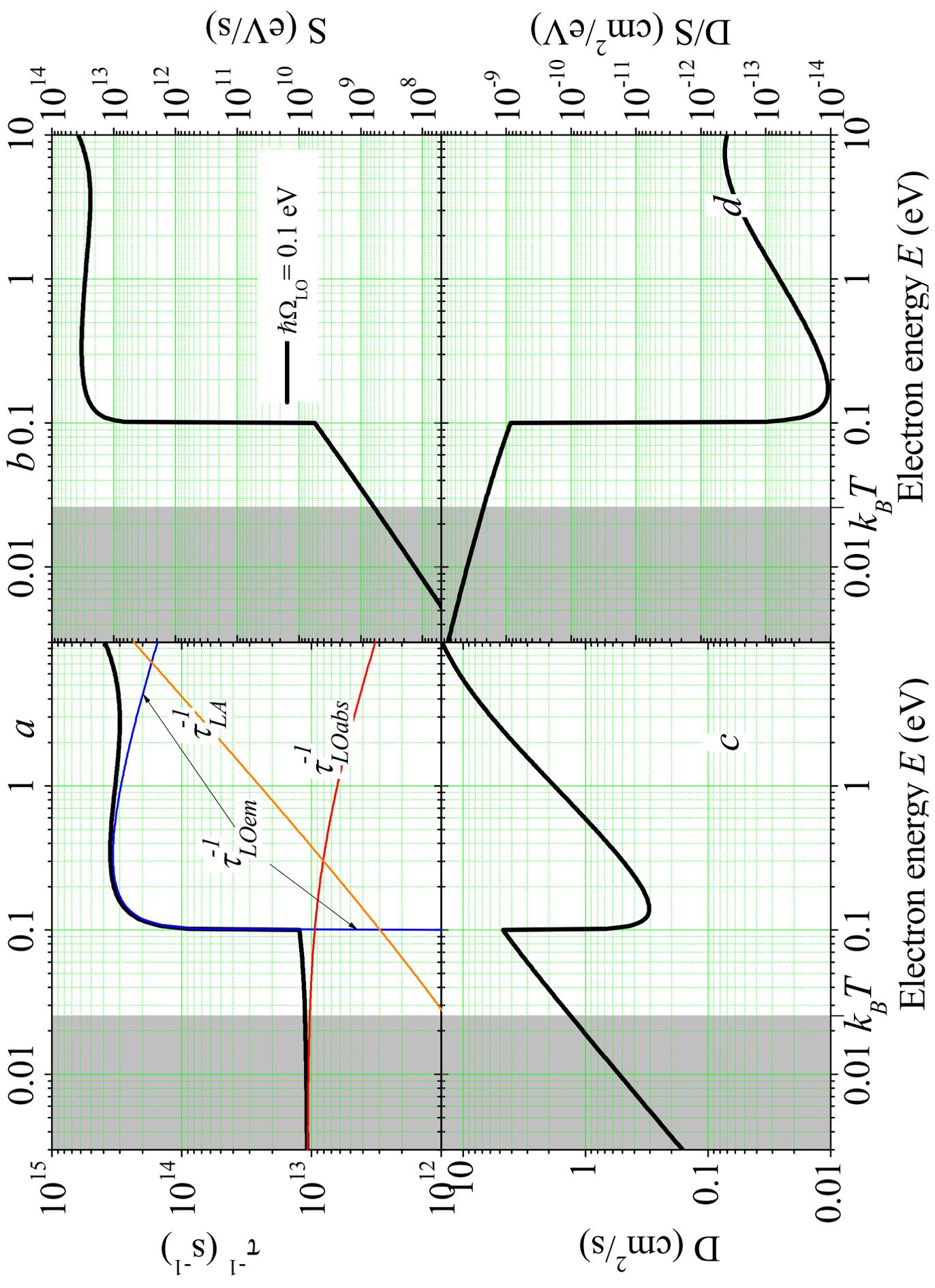


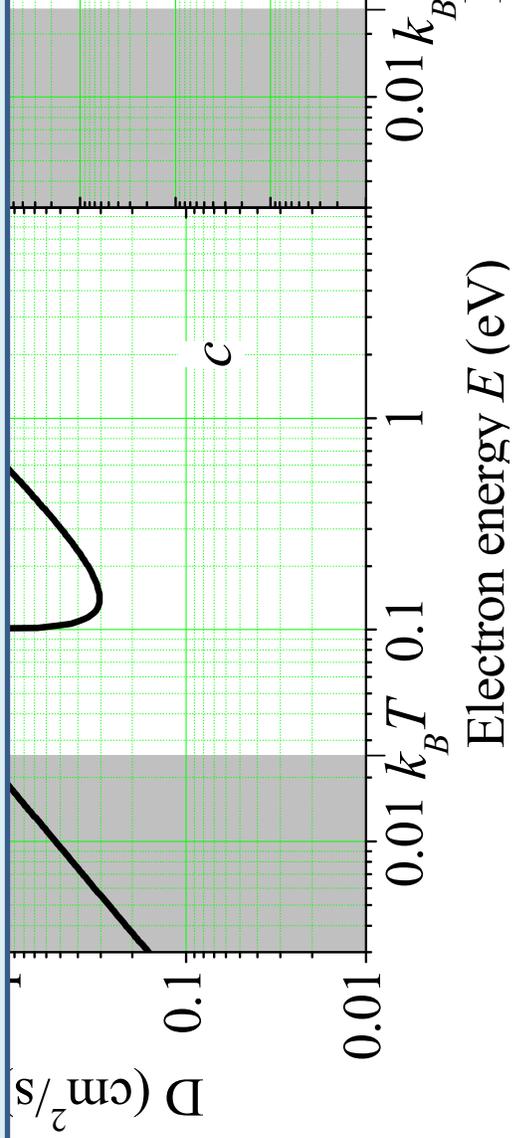
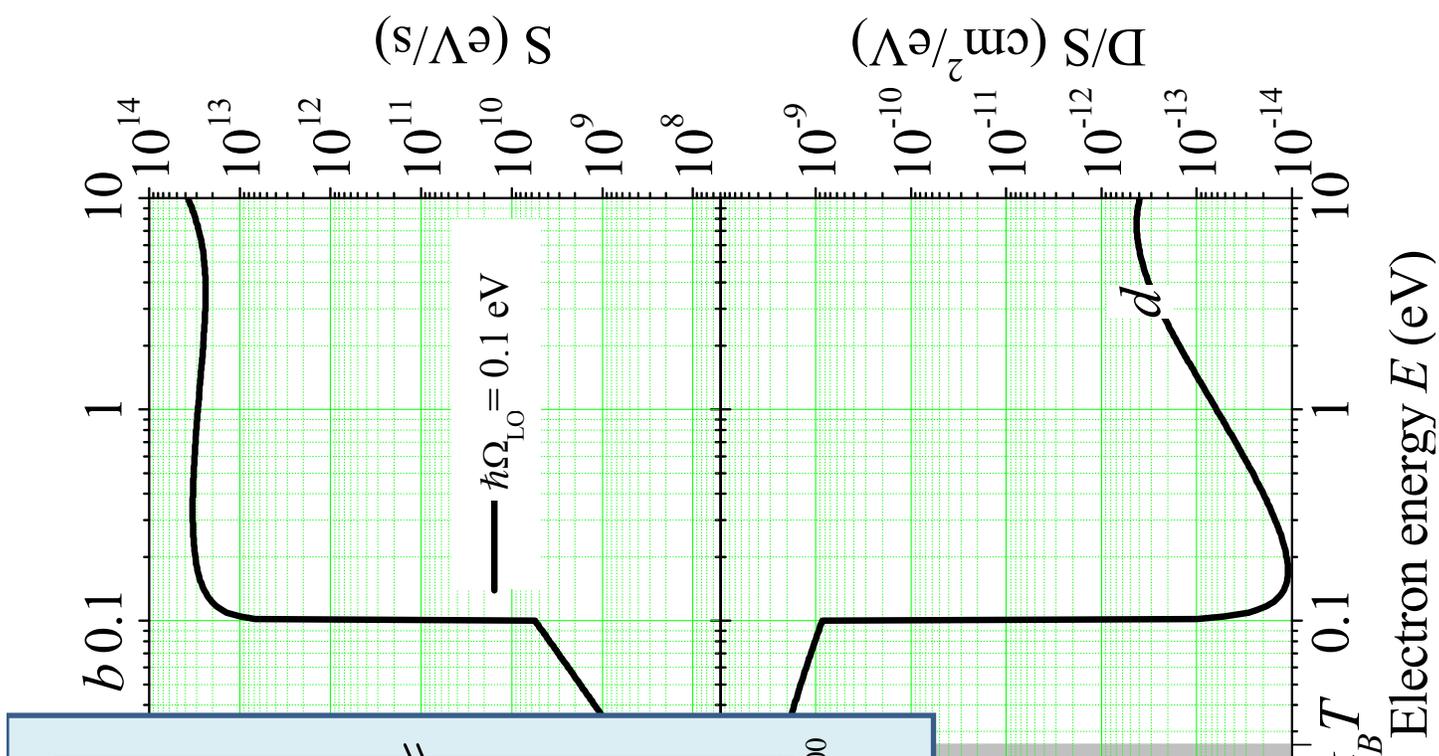
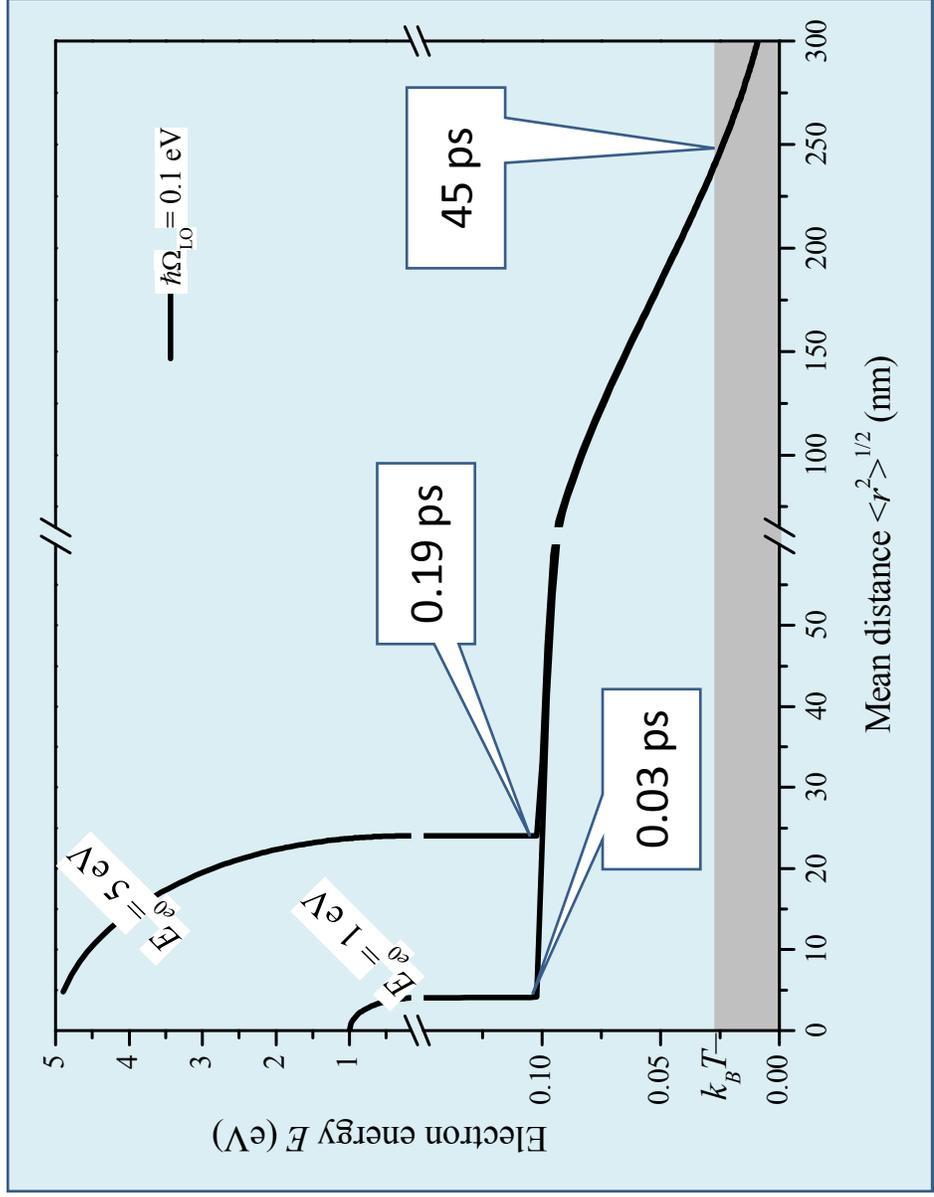
M.Kretov, A.Sherbinin, private communication

Different cases to discuss

R.Kirkin, V.V. Mikhailin, and A.N. Vasil'ev, *Recombination of correlated electron-hole pairs with account of hot capture with emission of optical phonons*, IEEE Transactions on Nuclear Science, vol. 59, issue 5, pp. 2057-2064 (2012)

- Simple oxide or fluoride (one LO branch)
 $\hbar\Omega_{LO} = 0.1 \text{ eV} > k_B T = 300\text{K} = 0.026 \text{ eV}$





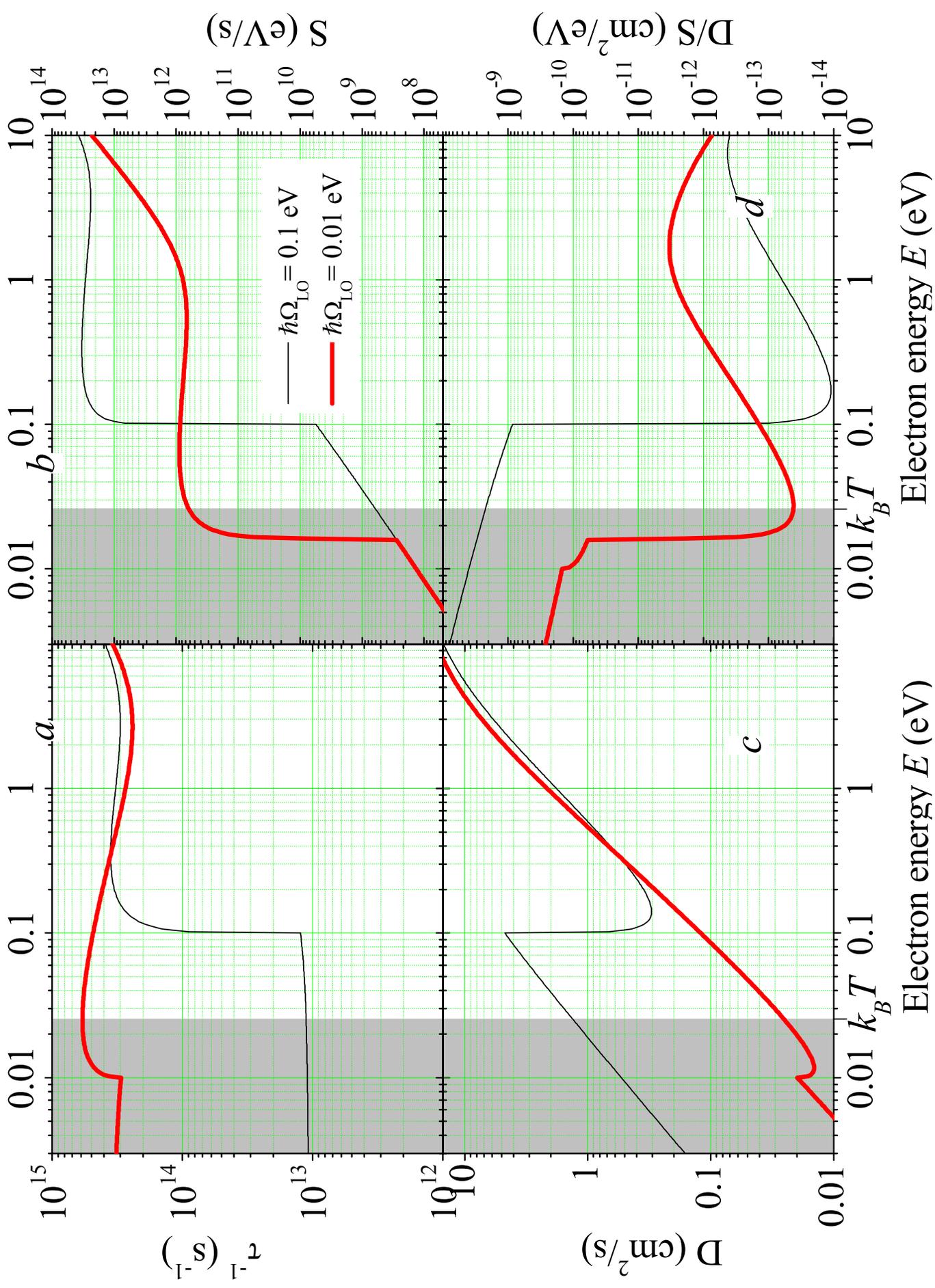
Different cases to discuss

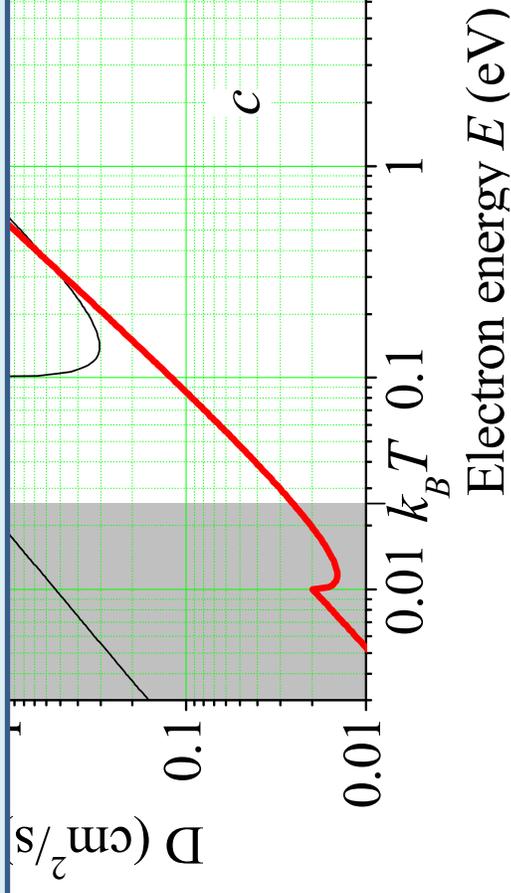
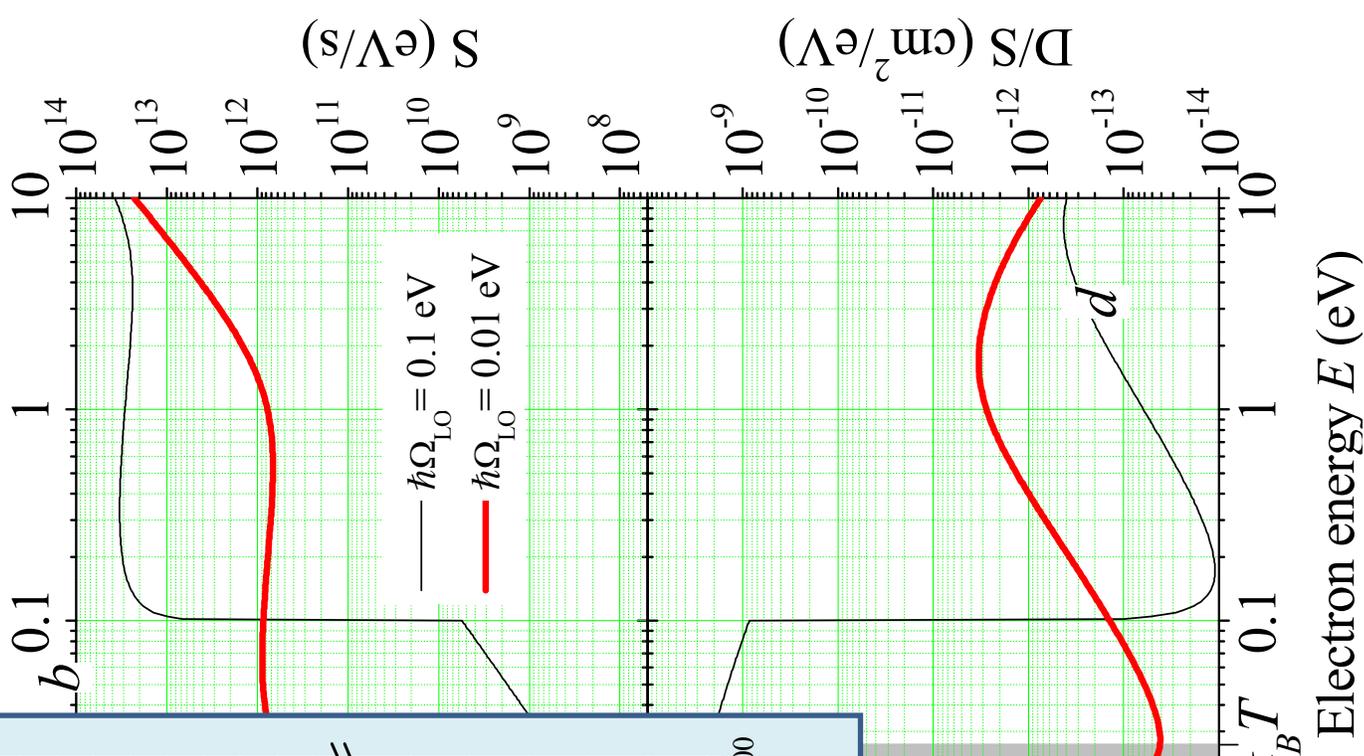
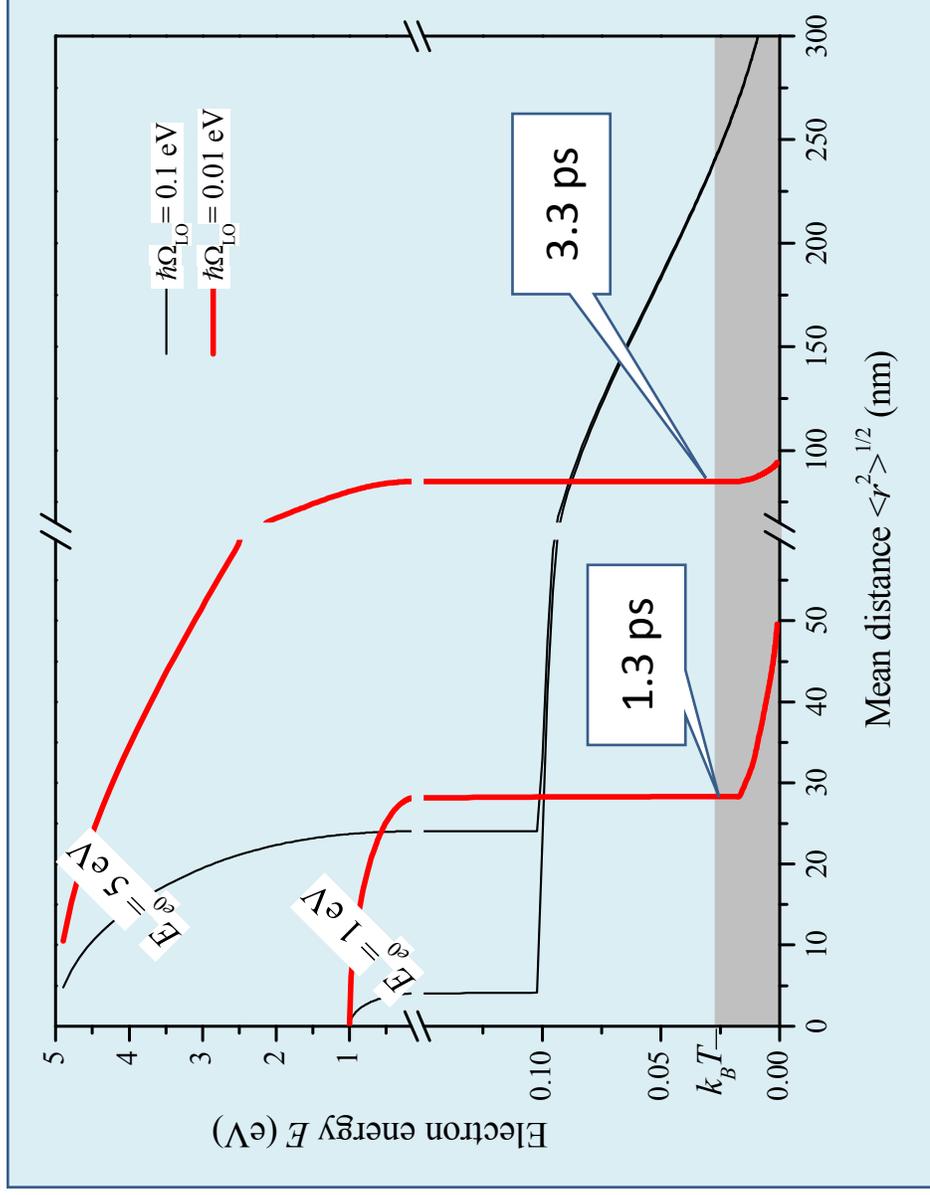
R.Kirkin, V.V. Mikhailin, and A.N. Vasil'ev, *Recombination of correlated electron-hole pairs with account of hot capture with emission of optical phonons*, IEEE Transactions on Nuclear Science, vol. 59, issue 5, pp. 2057-2064 (2012)

- Simple oxide or fluoride (one LO branch)
 $\hbar\Omega_{LO} = 0.1 \text{ eV} > k_B T = 300\text{K} = 0.026 \text{ eV}$

- Simple iodide (e.g. CsI, one LO branch)

$$\hbar\Omega_{LO} = 0.01 \text{ eV} < k_B T$$



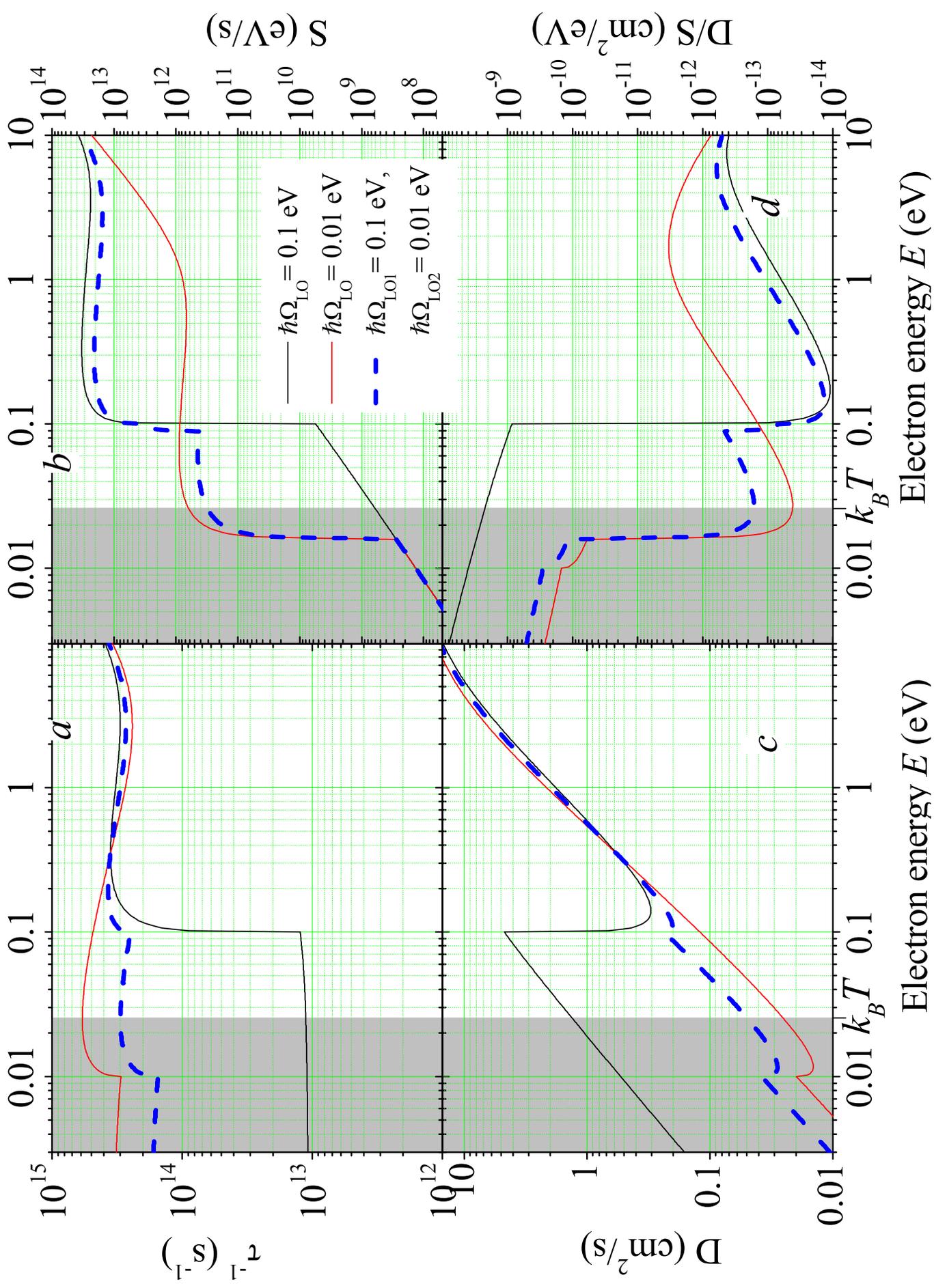


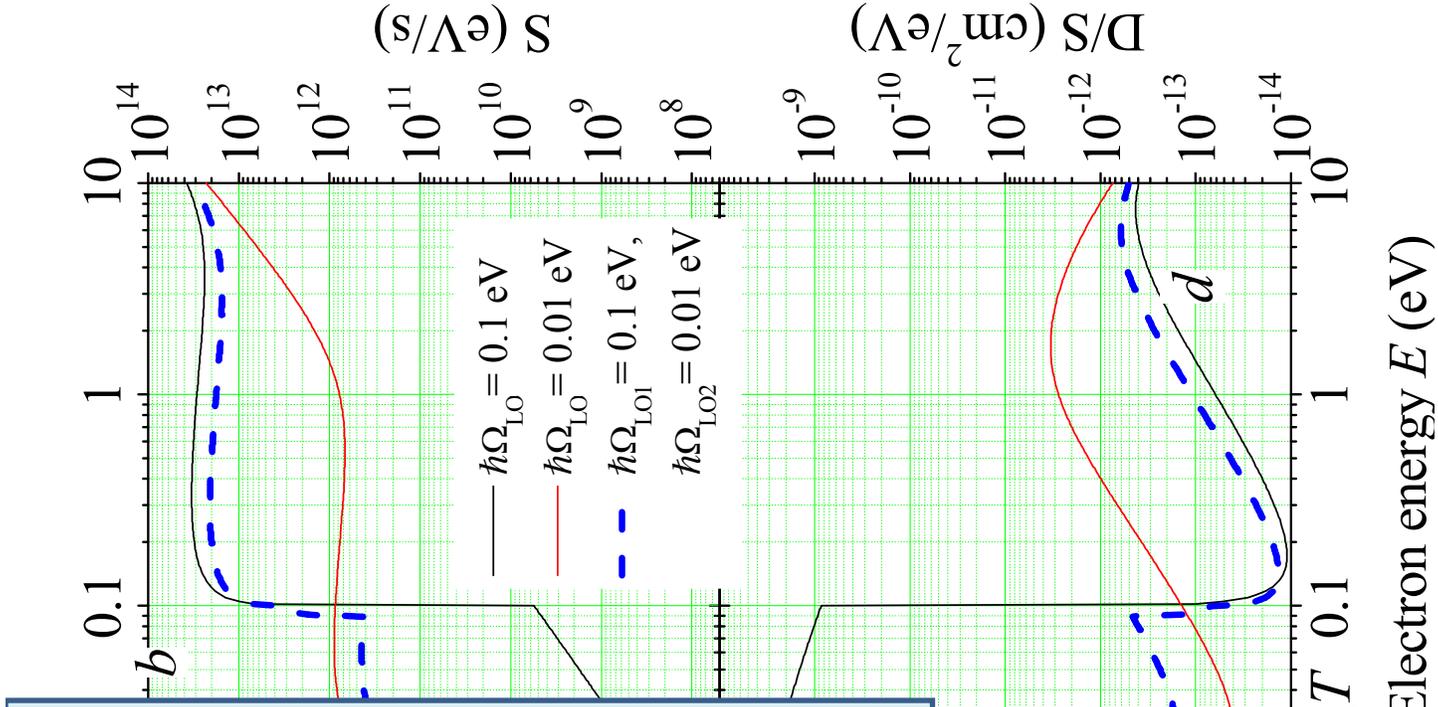
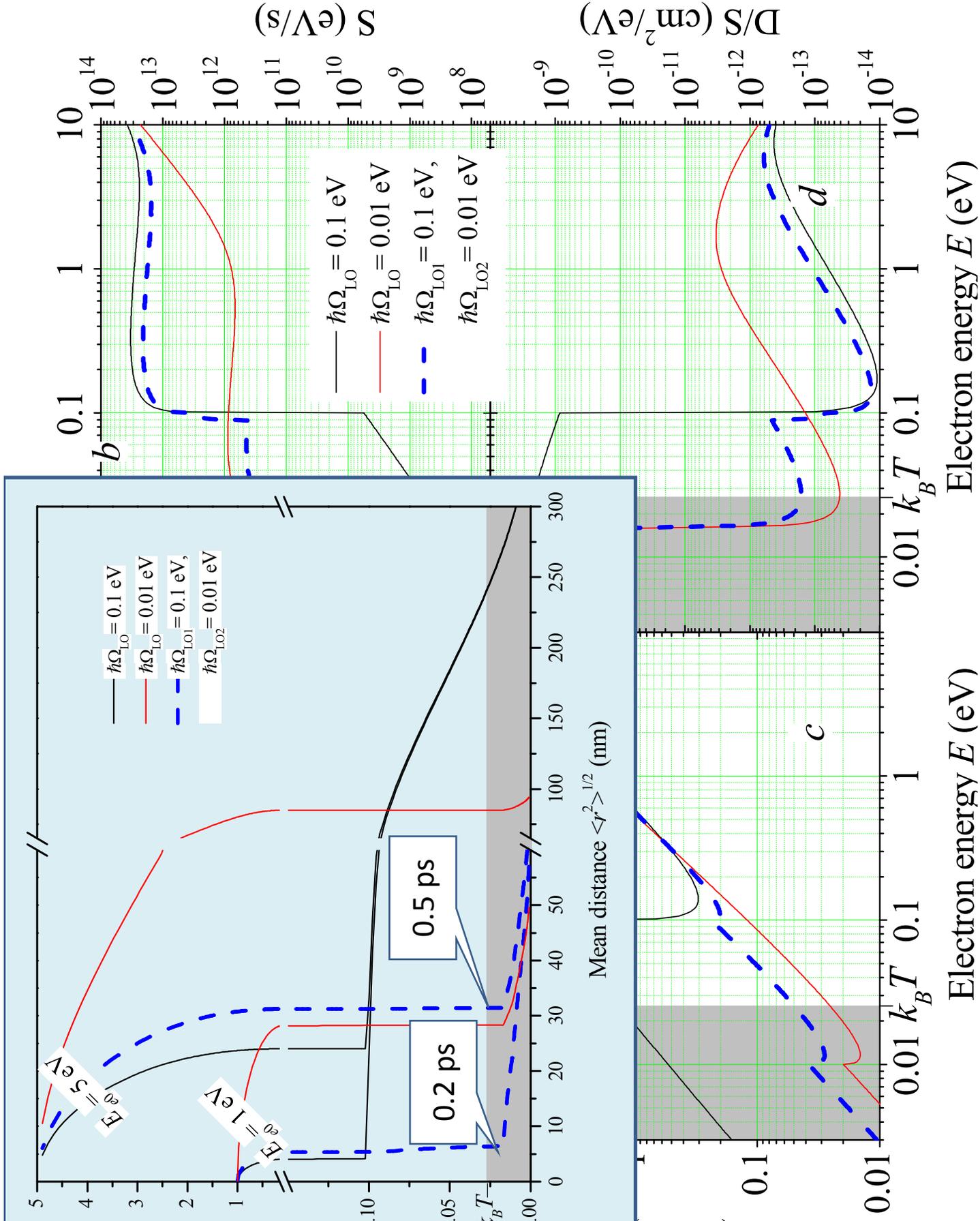
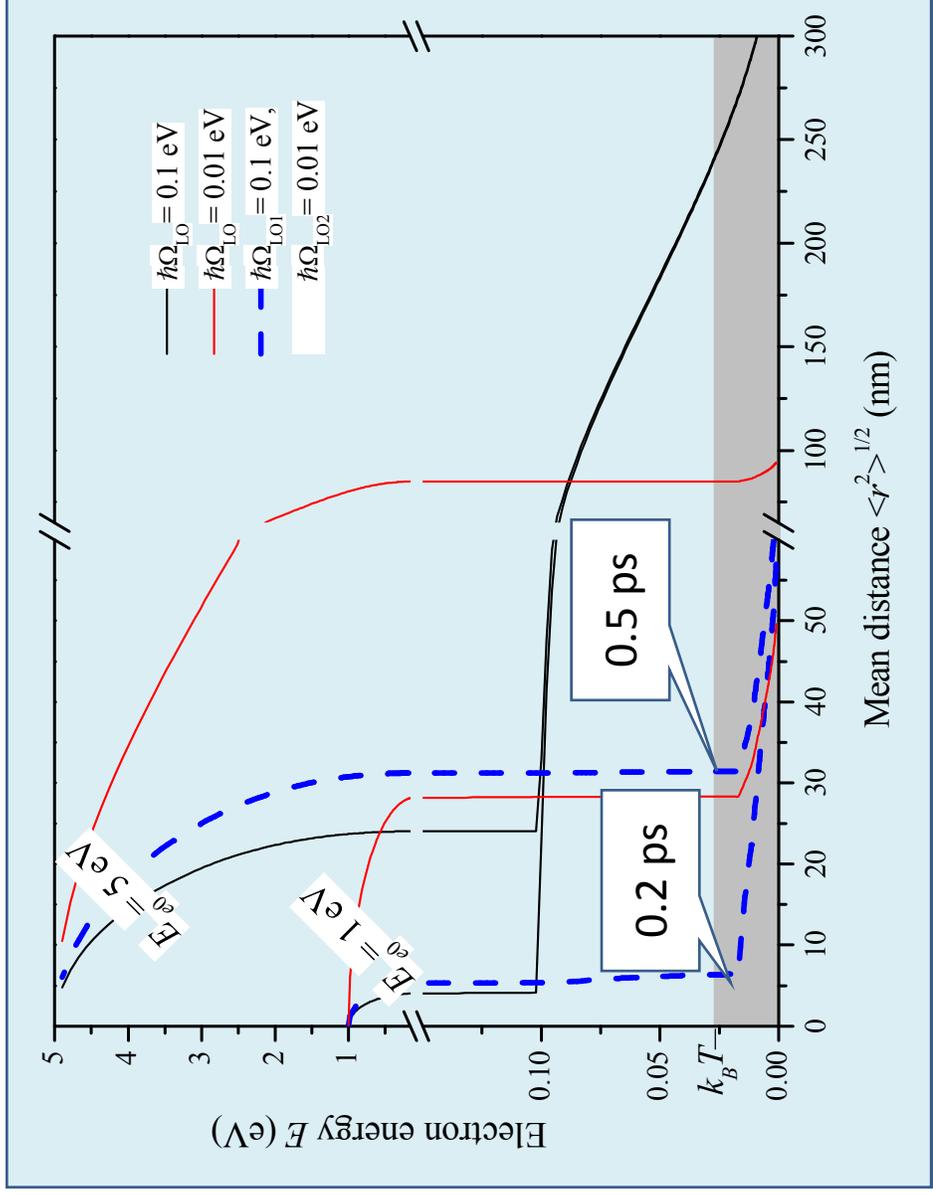
Different cases to discuss

R.Kirkin, V.V. Mikhailin, and A.N. Vasil'ev, *Recombination of correlated electron-hole pairs with account of hot capture with emission of optical phonons*, IEEE Transactions on Nuclear Science, vol. 59, issue 5, pp. 2057-2064 (2012)

- Simple oxide or fluoride (one LO branch)
 $\hbar\Omega_{LO} = 0.1 \text{ eV} > k_B T = 300\text{K} = 0.026 \text{ eV}$
- Simple iodide (e.g. CsI, one LO branch)
 $\hbar\Omega_{LO} = 0.01 \text{ eV} < k_B T$
- 2 LO branches with significantly different energies

$$\hbar\Omega_{LO1} = 0.1 \text{ eV}, \hbar\Omega_{LO2} = 0.01 \text{ eV}$$





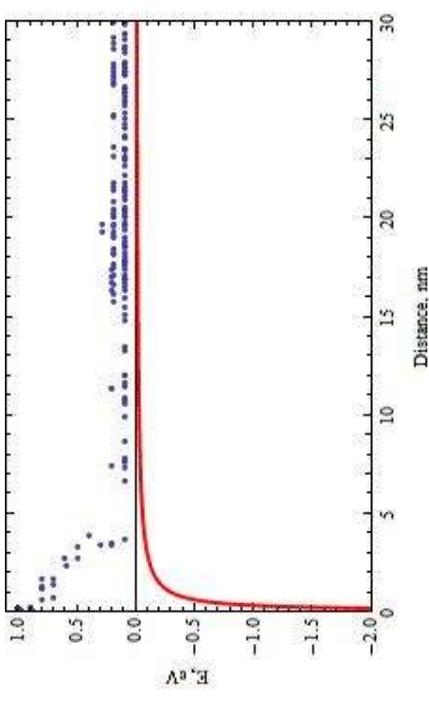
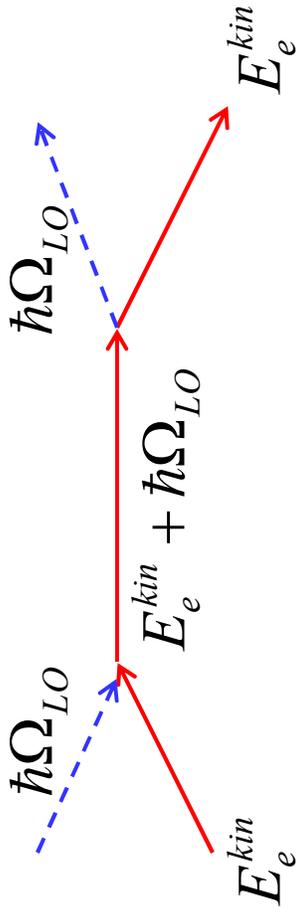
Different cases to discuss

R.Kirkin, V.V. Mikhailin, and A.N. Vasil'ev, *Recombination of correlated electron-hole pairs with account of hot capture with emission of optical phonons*, IEEE Transactions on Nuclear Science, vol. 59, issue 5, pp. 2057-2064 (2012)

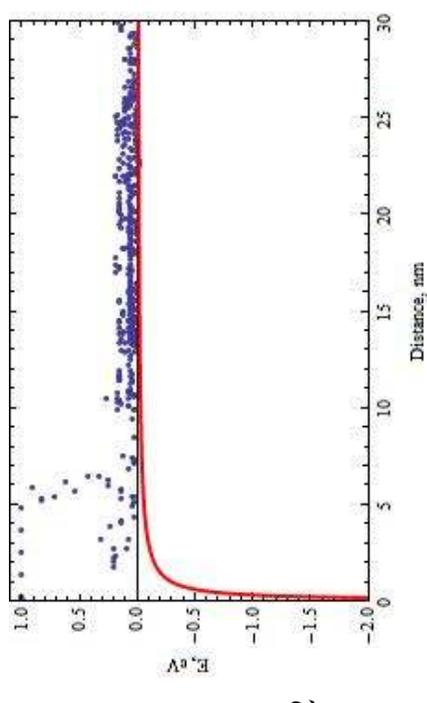
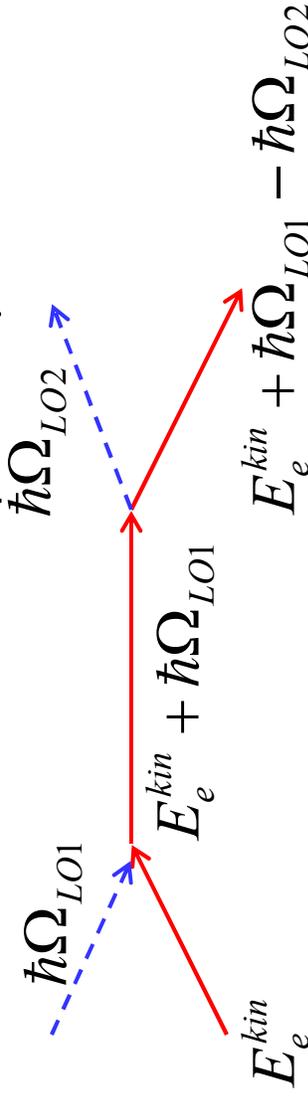
- Simple oxide or fluoride (one LO branch)
 $\hbar\Omega_{LO} = 0.1 \text{ eV} > k_B T = 300\text{K} = 0.026 \text{ eV}$
- Simple iodide (e.g. CsI, one LO branch)
 $\hbar\Omega_{LO} = 0.01 \text{ eV} < k_B T$
- 2 LO branches with significantly different energies
 $\hbar\Omega_{LO1} = 0.1 \text{ eV}, \hbar\Omega_{LO2} = 0.01 \text{ eV}$
- 2 LO branches with close energies
 $\hbar\Omega_{LO1} = 0.1 \text{ eV}, \hbar\Omega_{LO2} = 0.08 \text{ eV}$

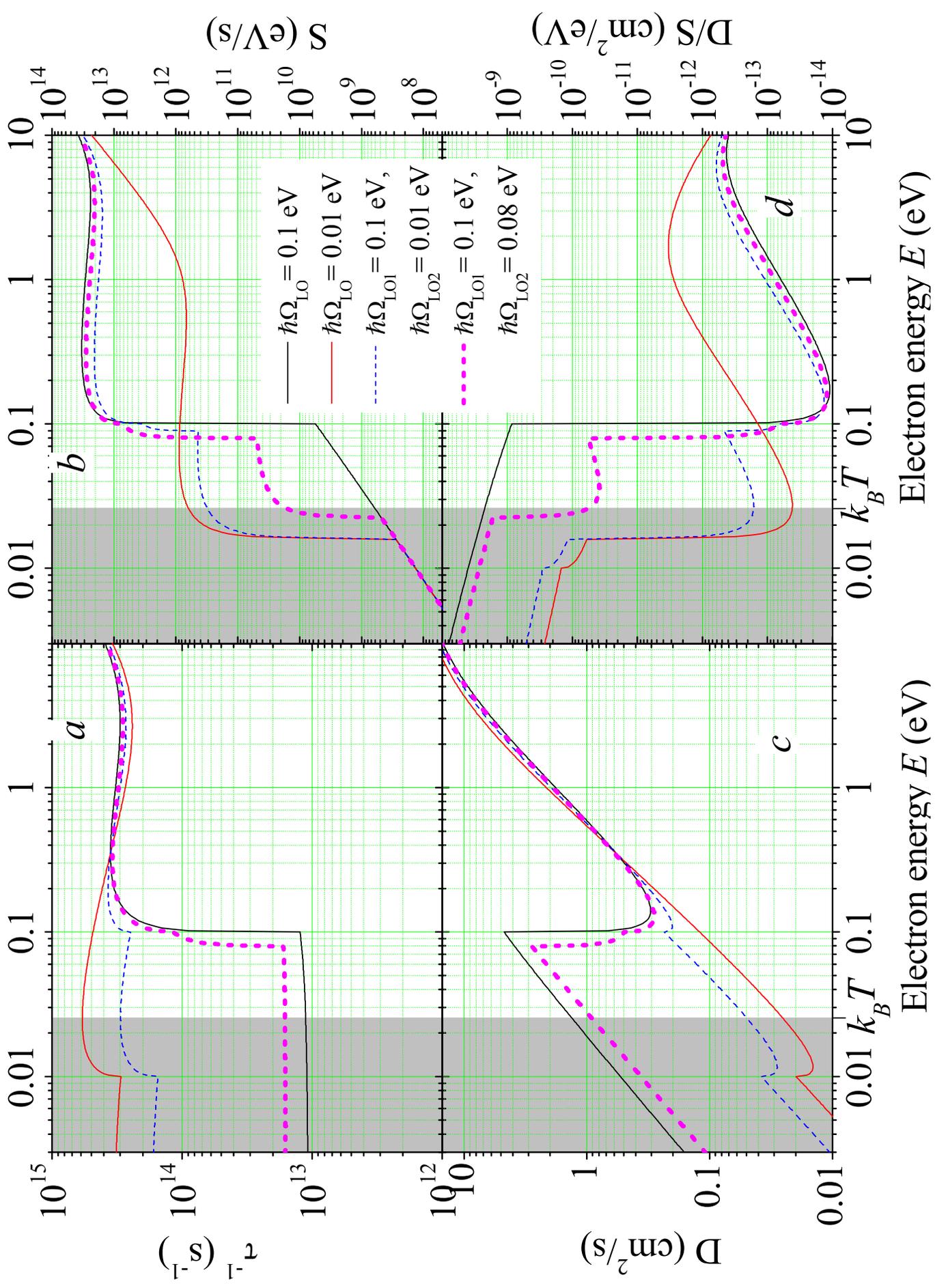
Interaction with LO phonons in LO-passive region

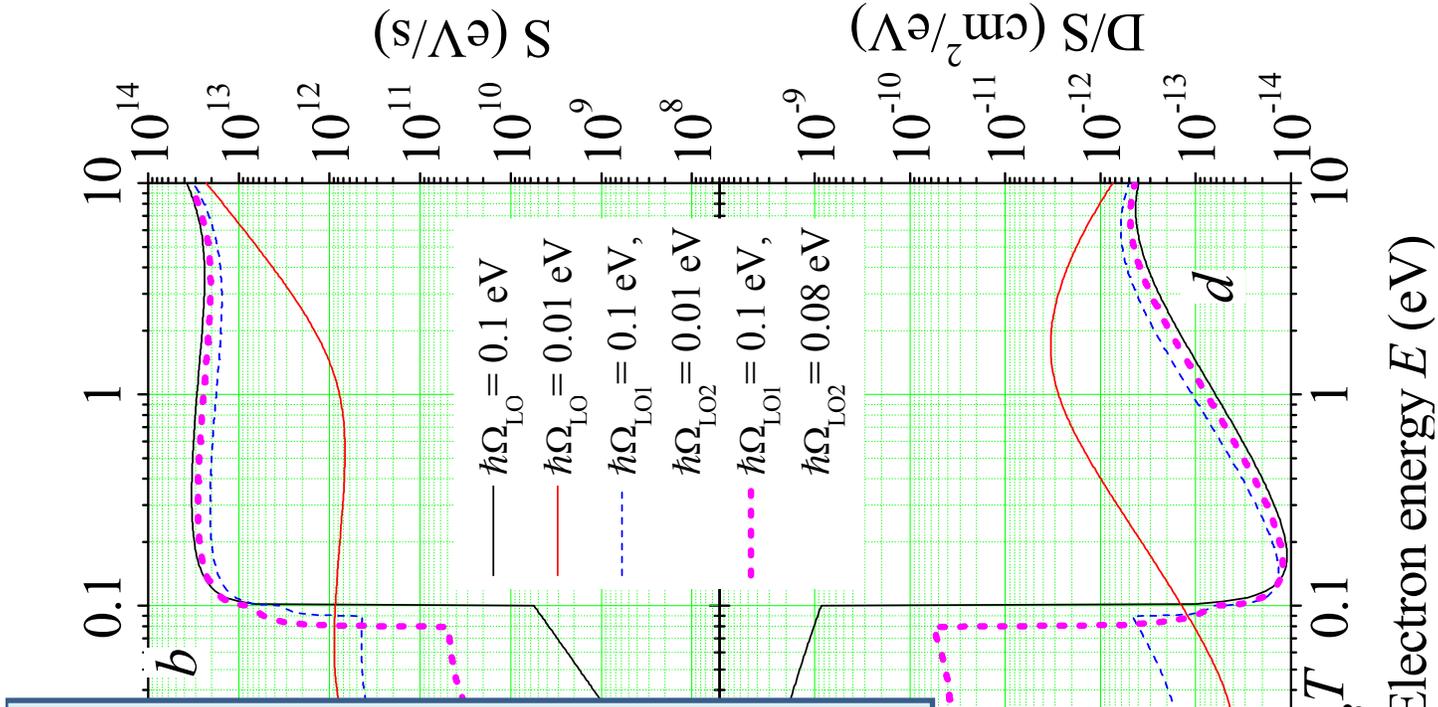
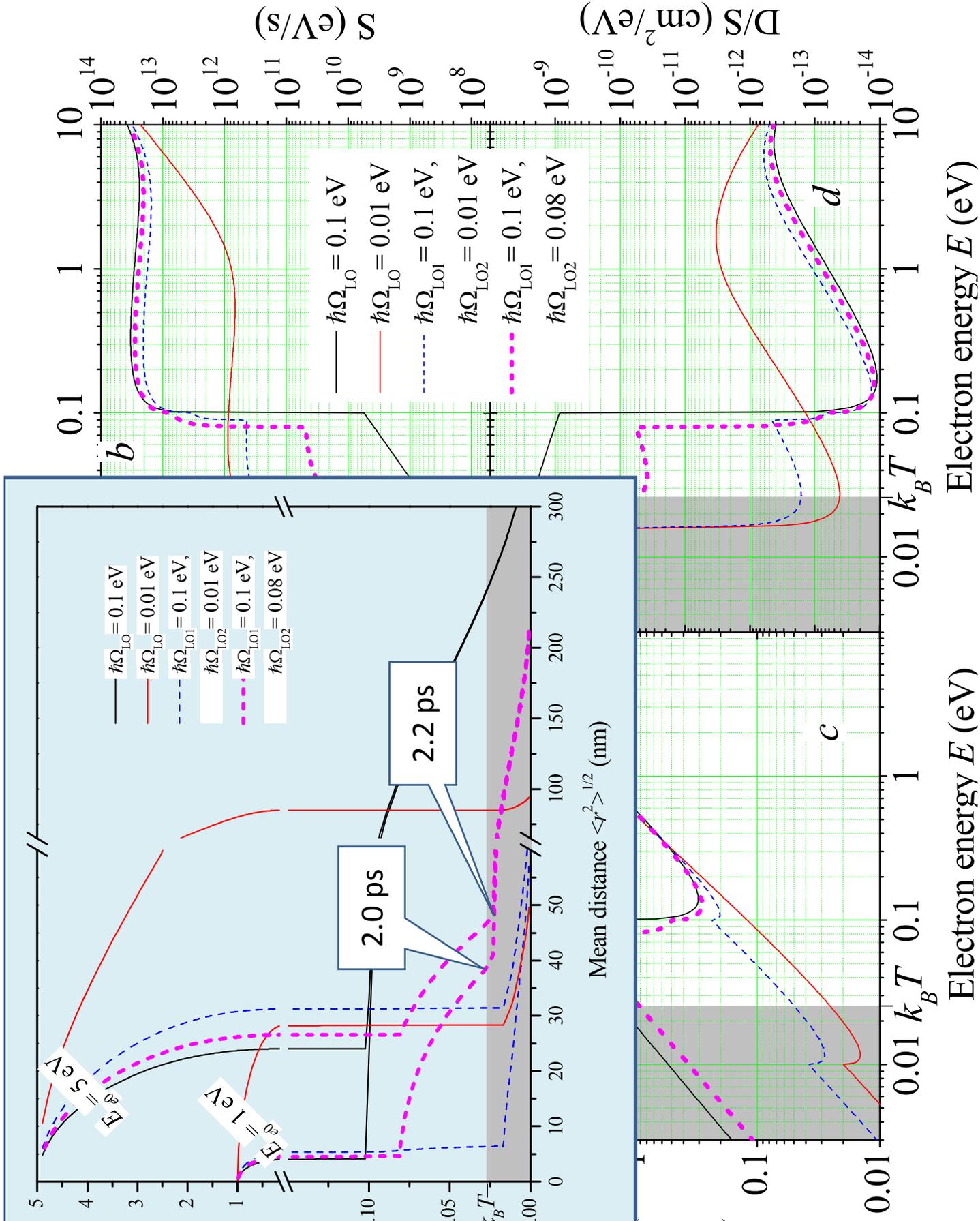
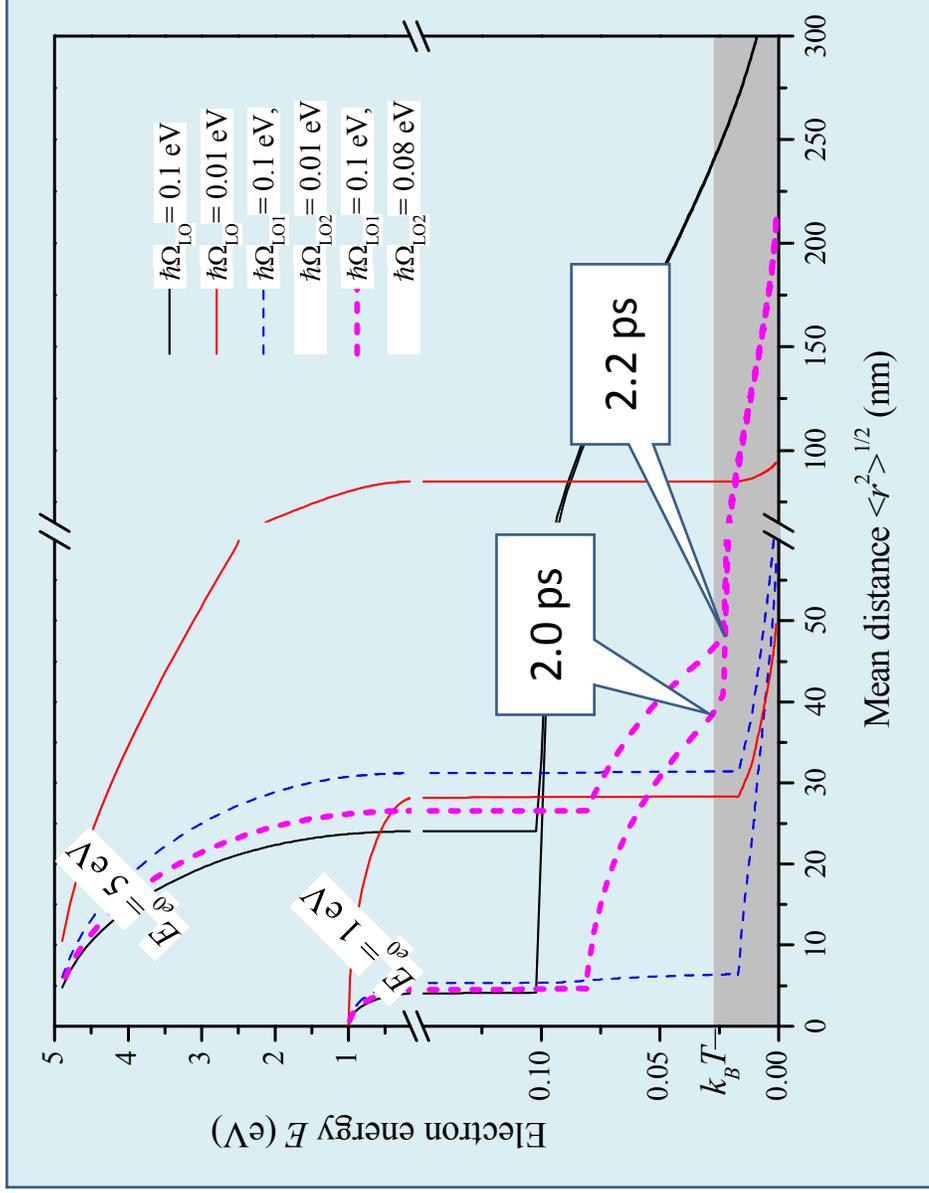
- One LO branch (2 atoms/unit cell) – Spatial diffusion is due to LO phonons, and energy relaxation is due to LA phonons)



Few LO branches (N atoms/cell) \rightarrow (N-1) PLO) (Both spatial diffusion and relaxation are due to LO phonons)







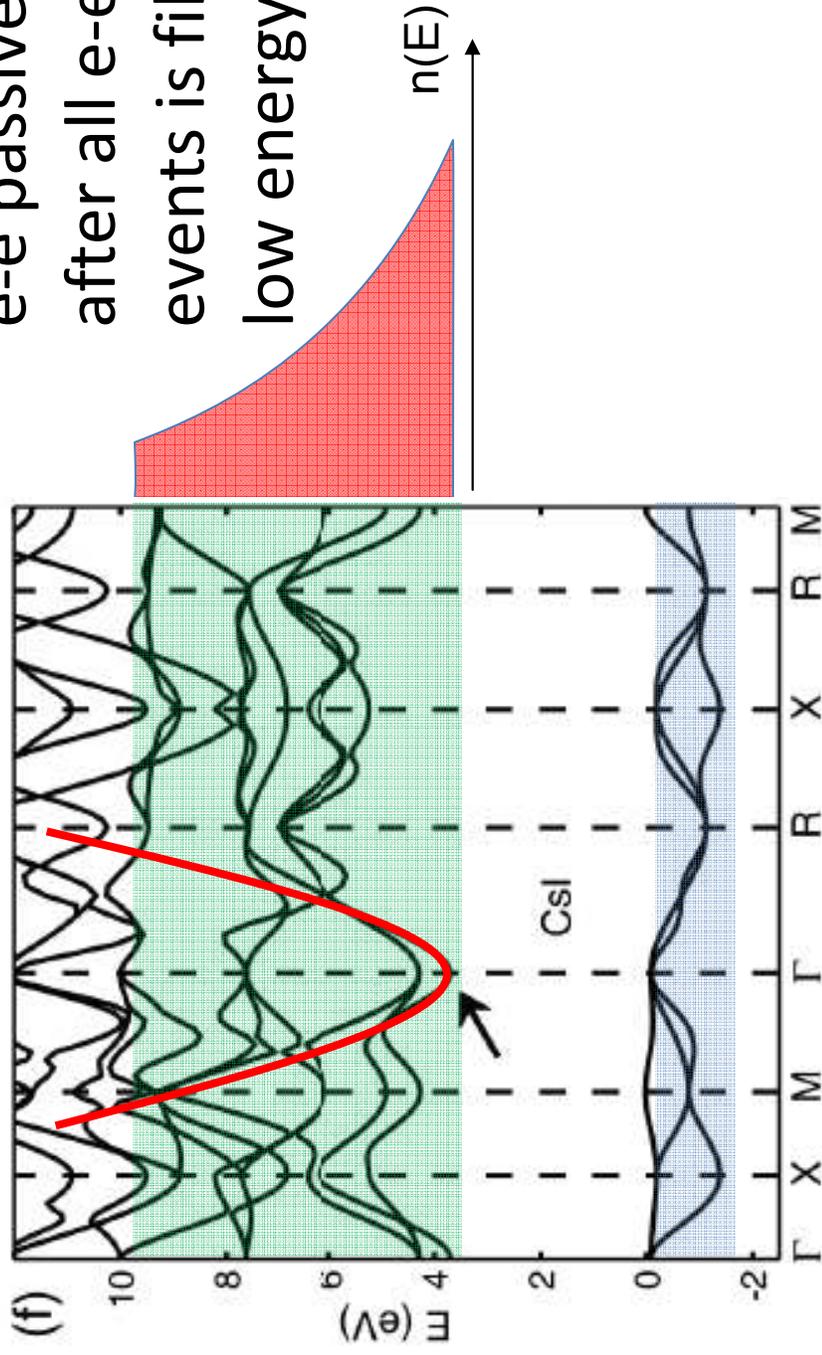
Outline

- Spatial scales for processes in scintillators
- Nanoparticles as scintillators
- Cascade, thermalization and recombination
- Different types of mobilities
- Thermalization length for different types of crystals
- **Interconnection of cascade, thermalization and recombination stages in binary iodides**
- Why cascade is so effective in CsI?
- Thermalization length and impurities
- Concluding remarks

Starting states for thermalization ($E_{\text{kin}} < E_g$)

Band structure calculations

from W. Setyawan, R. M. Gaume et al. *IEEE TNS*, 2009



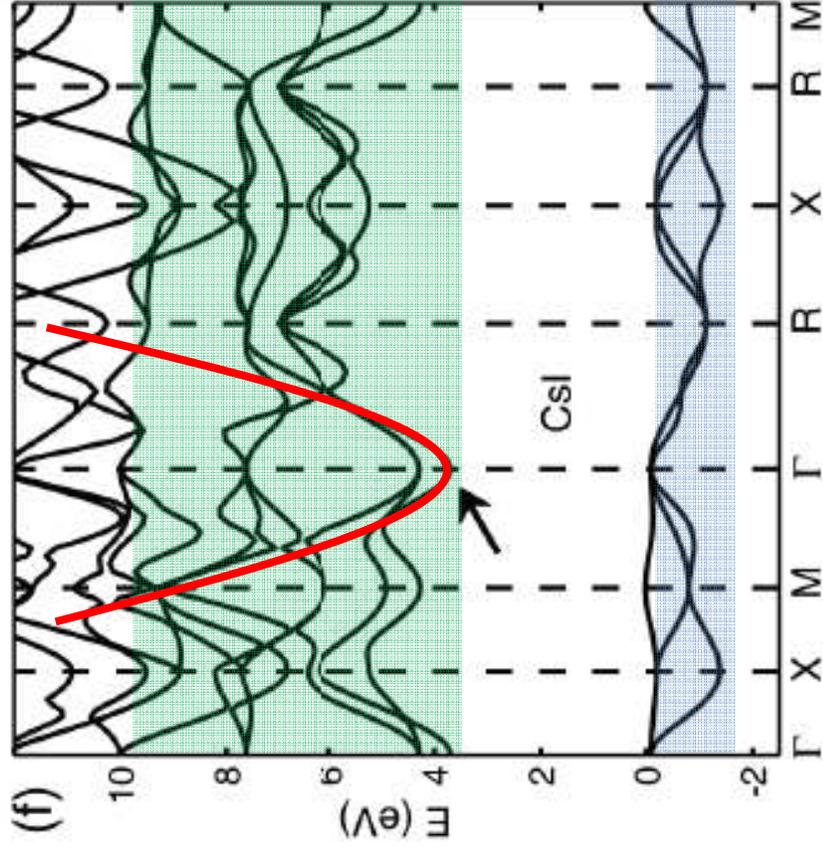
e-e passive region in CB
after all e-e scattering
events is filled mostly in
low energy part

Starting states for thermalization

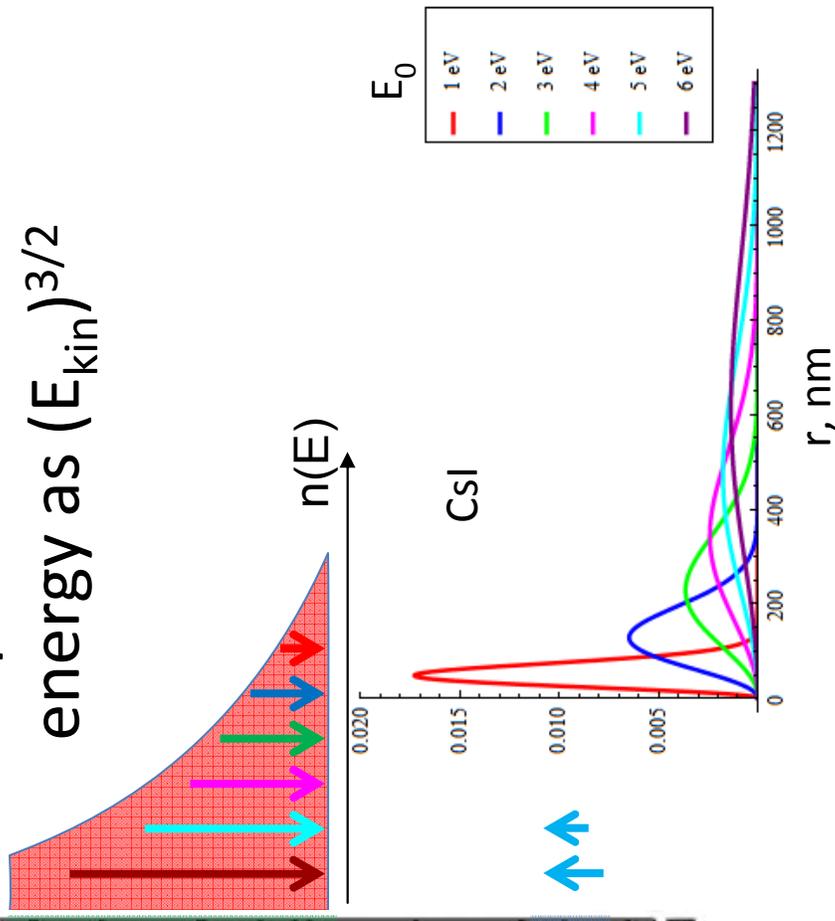
$$(E_{\text{kin}} < E_{\text{g}})$$

Band structure calculations

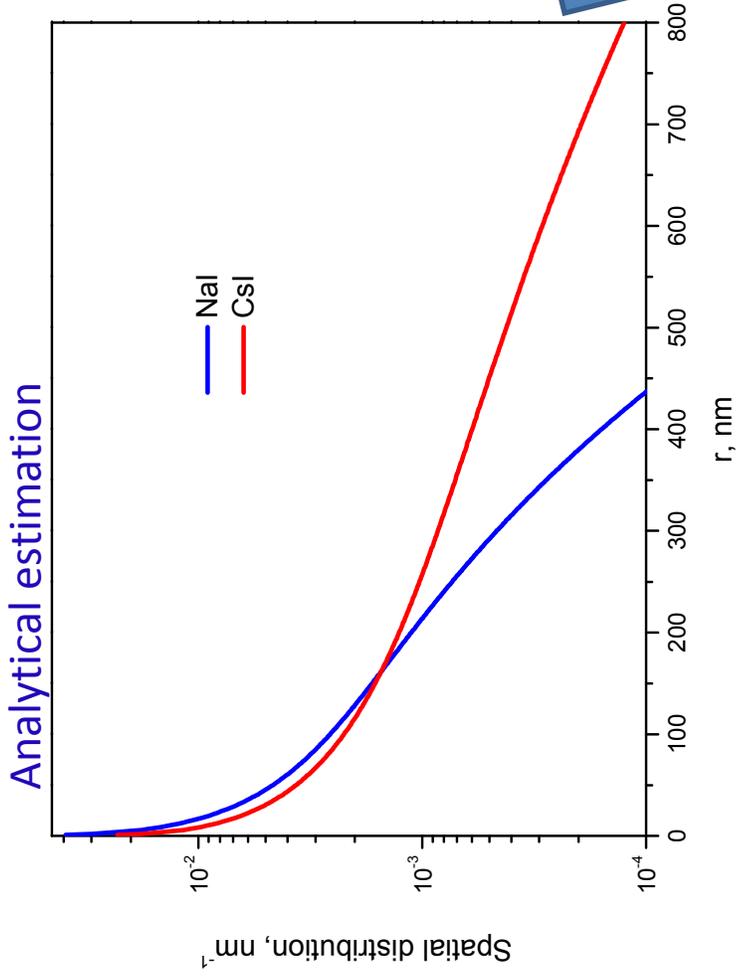
from W. Setyawan, R. M. Gaume et al. *IEEE TNS*, 2009



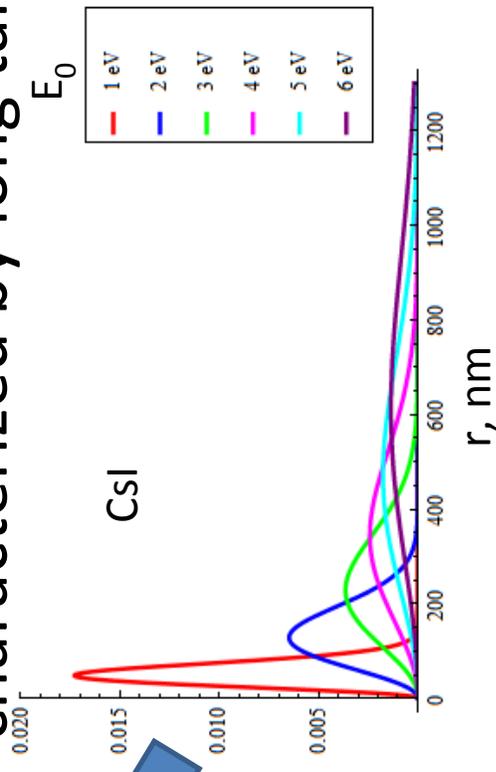
Thermalization length depends on kinetic energy as $(E_{\text{kin}})^{3/2}$



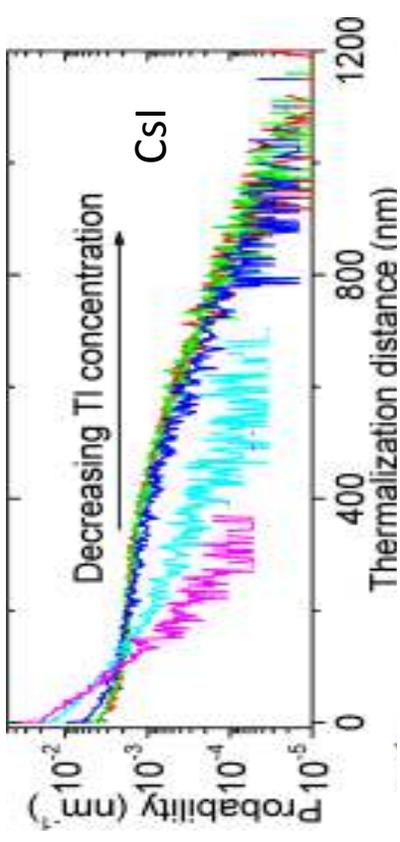
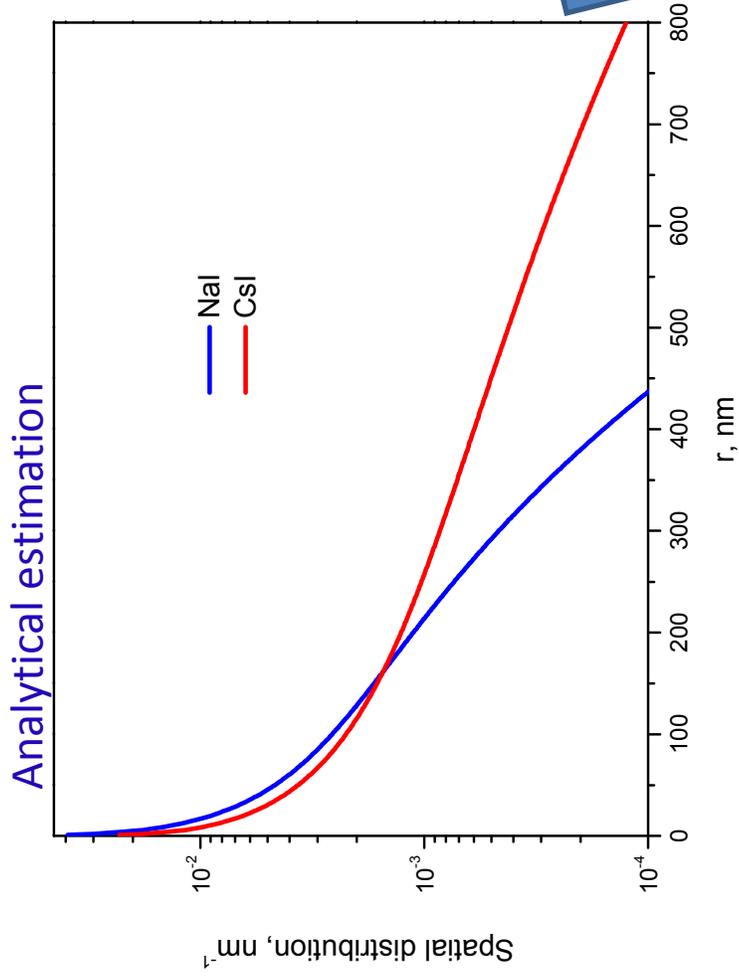
Spatial distribution of thermalized electrons



The resulting spatial distributions of excitations after thermalization is non-Gaussian and is characterized by long tail

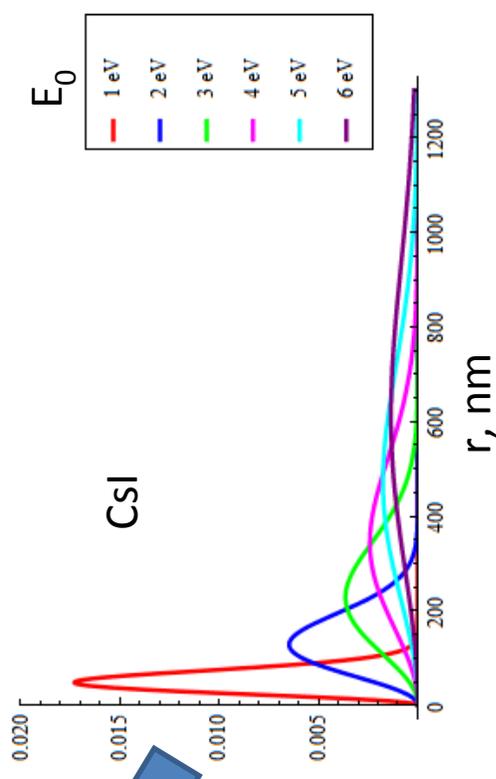


Spatial distribution of thermalized electrons

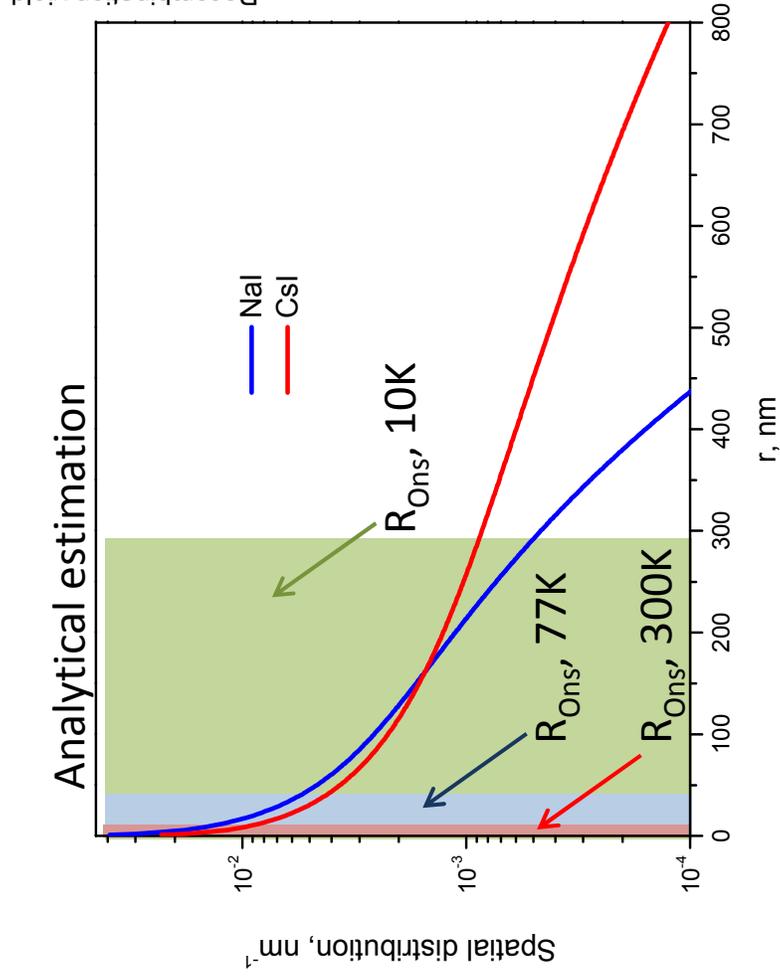


Computer simulation of electron thermalization in CsI and CsI(Tl),

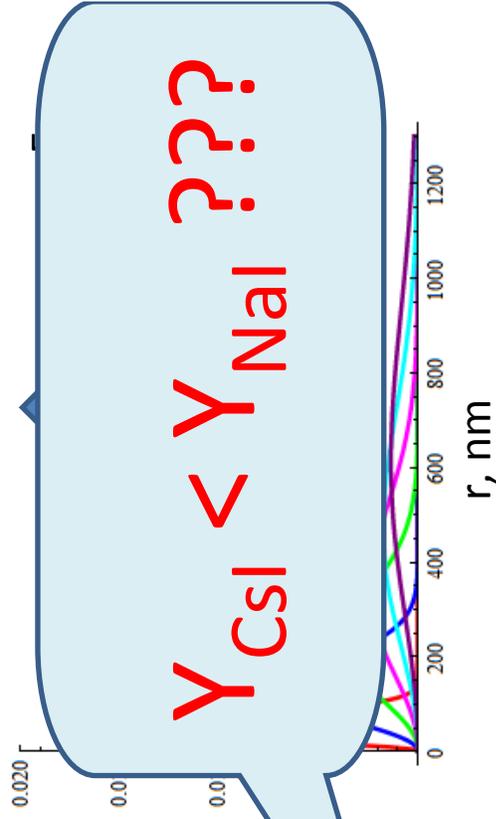
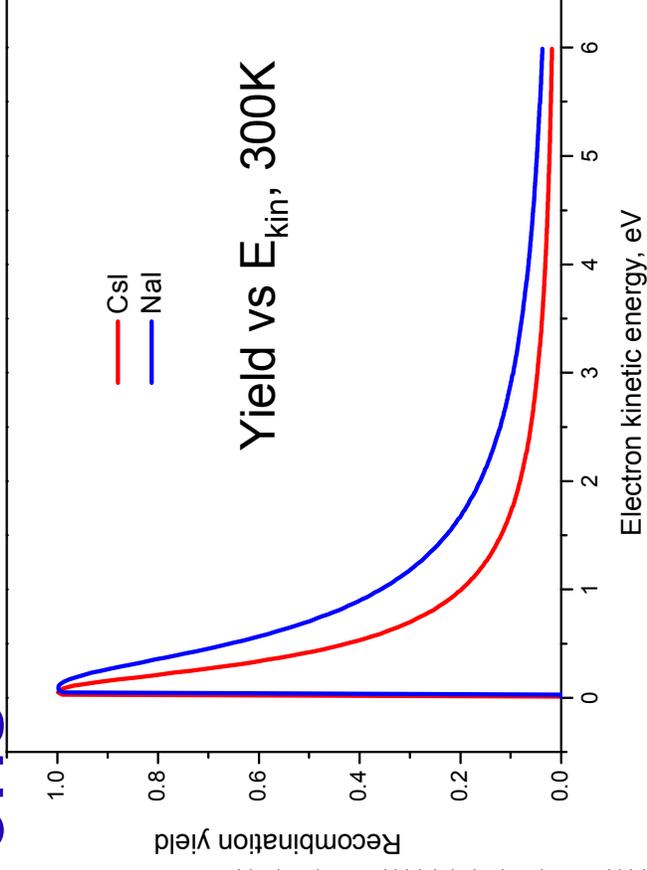
Z. Wang, Y. Xie, B. D. Cannon et al. 2011



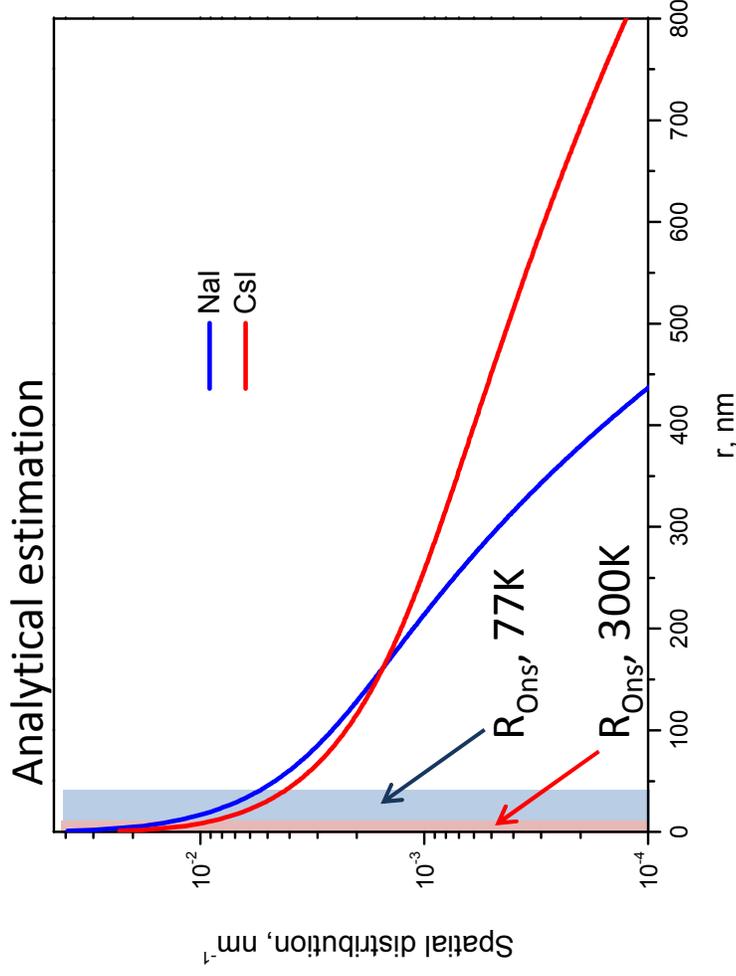
Spatial distribution of thermalized electrons



	$R_{Ons'}$, 300K	Yield, 300K	Yield, 77K
CsI	9.87 nm	0.24	0.44
NaI	9.05 nm	0.34	0.58



Spatial distribution of thermalized electrons



	$R_{\text{ons}}, 300\text{K}$	Yield, 300K	Yield, 77K
CsI	9.87 nm	0.24	0.44
NaI	9.05 nm	0.34	0.58

$Y_{\text{CsI}} < Y_{\text{NaI}}$
 ????

Outline

- Spatial scales for processes in scintillators
- Nanoparticles as scintillators
- Cascade, thermalization and recombination
- Different types of mobilities
- Thermalization length for different types of crystals
- Interconnection of cascade, thermalization and recombination stages in binary iodides
- **Why cascade is so effective in CsI?**
- Thermalization length and impurities
- Concluding remarks

Transitions from 5pCs core levels

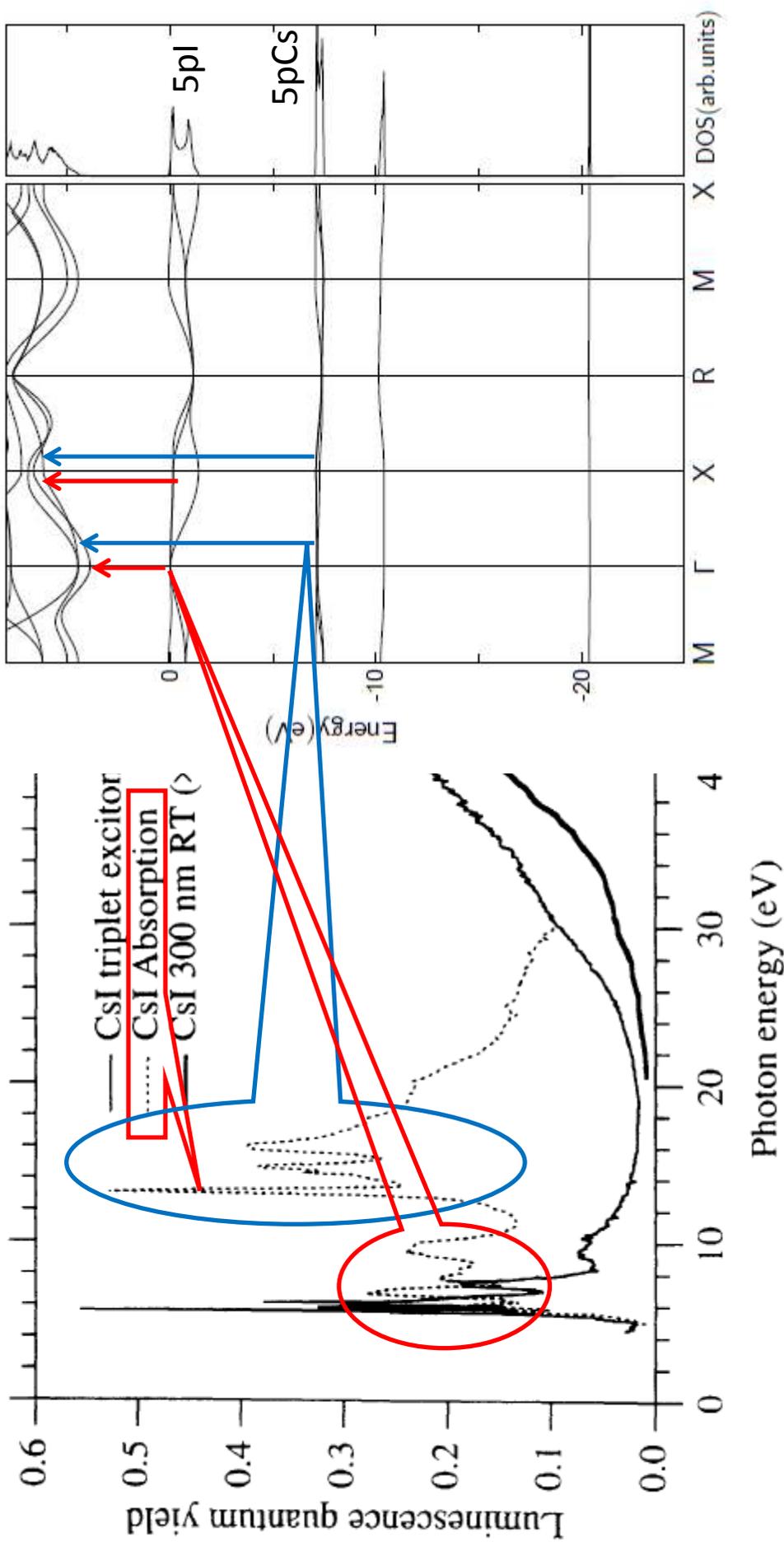
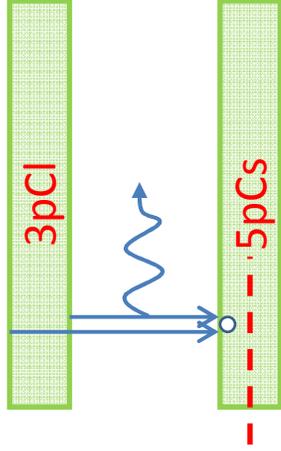


FIG. 2. Excitation spectra of CsI luminescence: the FIL (300 K) (thick) and of triplet exciton (100 K) (thin) compared with CsI absorption (dashed).

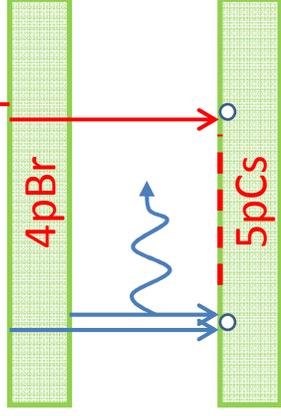
From core-valence transitions to Auger process

in cesium halides



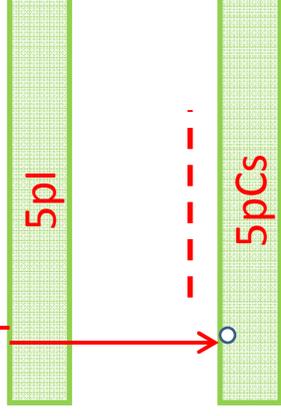
CsCl

Radiative decay
of 5p core hole



CsBr

Radiative and Auger
decay of 5p core hole



CsI

Auger decay of 5pI core
hole with creation of
exciton or low-energy
e-h pair ($E_{kin} < 1 \text{ eV}$)

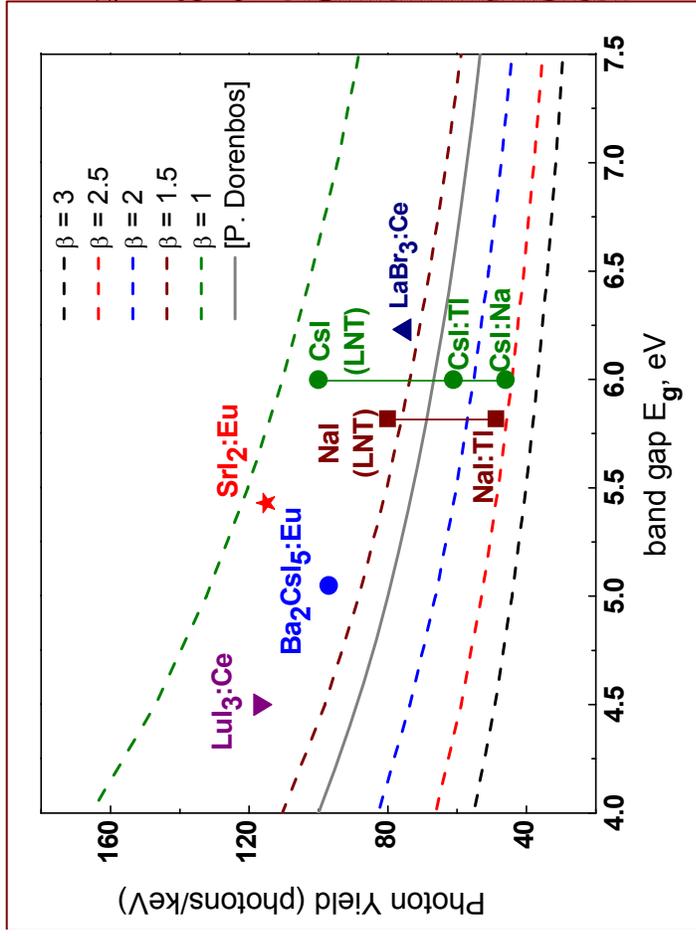


NaI

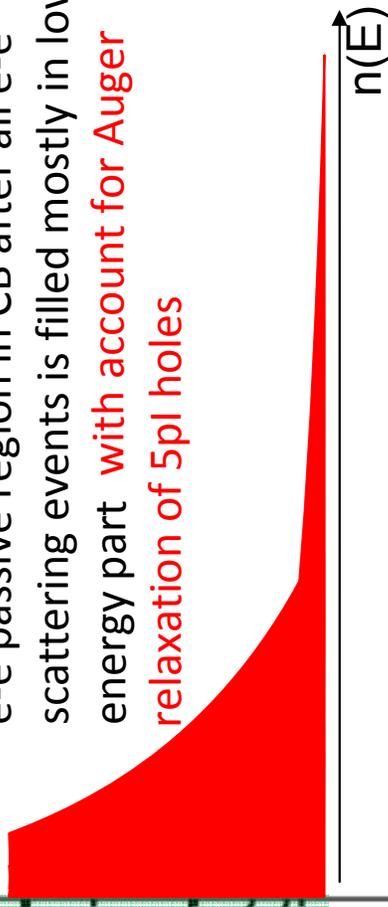
No uppermost core
levels

Starting states for thermalization

$$(E_{\text{kin}} < E_{\text{g}})$$



e-e passive region in CB after all e-e scattering events is filled mostly in low energy part **with account for Auger relaxation of 5pl holes**



Estimation of β decreases significantly!
 Creation of each 5pl hole with threshold energy 13 eV produces 2 e-h pairs, one electron and both holes of which has low kinetic energy!

Outline

- Spatial scales for processes in scintillators
- Nanoparticles as scintillators
- Cascade, thermalization and recombination
- Different types of mobilities
- Thermalization length for different types of crystals
- Interconnection of cascade, thermalization and recombination stages in binary iodides
- Why cascade is so effective in CsI?
- **Thermalization length and impurities**
- Concluding remarks

Elastic scattering on impurities and carriers

$$\frac{1}{\tau} = \nu \sigma N = \sqrt{\frac{2E}{m^*}} \sigma N$$

Charged impurities/carriers: Conwell & Weisskopf (Phys. Rev. 77, 388-390, 1950)

$$\sigma_c^{CW} = 2\pi \left(\frac{Ze^2}{4\pi\epsilon_0\epsilon_{st}2E} \right)^2 \ln \left(1 + 4 \left(\frac{E}{E_m} \right)^2 \right), \quad E_m = \frac{Ze^2}{4\pi\epsilon_0\epsilon_{st}m}, \quad r_m = \frac{1}{2} n_c^{-1/3}$$

$$\sigma_c^{CW} = \frac{1}{2} \pi R_{Oms}^2 \left(\frac{k_B T}{E} \right)^2 \ln \left(1 + \left(\frac{E}{k_B T x_m} \right)^2 \right), \quad x_m = R_{Oms} n_c^{1/3}$$

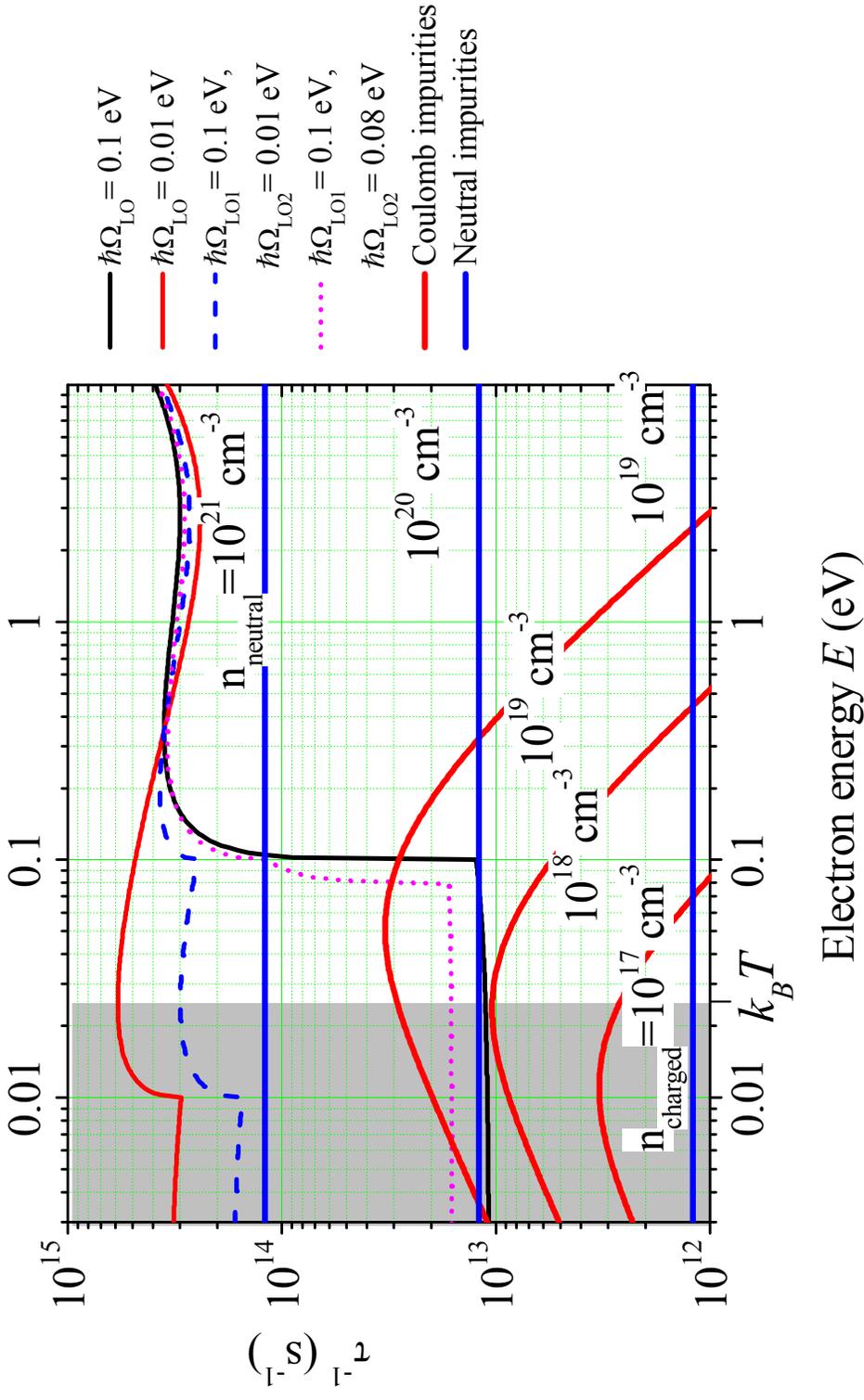
$$\frac{1}{\tau} = \sqrt{\frac{2k_B T}{m^*}} \frac{1}{2} \pi R_{Oms}^2 \left(\frac{k_B T}{E} \right)^{3/2} \ln \left(1 + \left(\frac{E}{k_B T x_m} \right)^2 \right) n_c = 1.5 \times 10^{-5} \left(\frac{k_B T}{E} \right)^{3/2} \ln \left(1 + \left(\frac{E}{k_B T x_m} \right)^2 \right) n_c [\text{cm}^{-3}] \frac{1}{s}$$

Neutral impurities

$$\sigma \approx 20 \frac{ka^*}{k^2}, \quad k = \frac{1}{\hbar} \sqrt{2m^*E}, \quad a^* - \text{impurity Bohr radius}$$

$$\sigma \approx \frac{20a^*\hbar}{\sqrt{2m^*E}}, \quad \frac{1}{\tau} = \frac{20a^*\hbar}{m^*} n = 1.2 \times 10^{-7} n [\text{cm}^{-3}] \frac{1}{s} = 1.2 \times 10^{13} n [\text{mol.}\%] \frac{1}{s} \quad (a^* = 1\text{nm}, m^* = m_e)$$

Elastic scattering on impurities and carriers



Scattering on impurities is the limiting factor for thermalization length only for crystals with high LO phonon energies in LO-passive region for high concentrations of neutral (>0.5%) impurities and for high concentration of carriers (>10¹⁸ cm⁻³)

Conclusions

The efficiency of recombination of geminate electron-hole pairs (high-energy part of electron track) depends on the energy of LO phonons and the number of LO phonon branches characterized by polarization interaction with electrons and holes:

- low yield in case of one LO branch with any energy (except for very heavy carrier masses) – both binary halides and binary oxides
- higher yield in the case of multiple LO branches with low energies – complex halides with many atoms in elementary cell
- high yield in case of multiple LO branches with wide spread of energies – complex oxides and crystals with oxyanions

Conclusions

The development of comprehensive model of scintillator based on multi-particle consideration of multi-scale evolution of strongly non-equilibrium excited region on the basis of deep directional experimental investigations allows to

- Make a progress in fundamental physics
- Obtain new results in applied physics – e.g. by justification that mixed crystals is a way to improve scintillator properties
- Be useful in pragmatic sense, because it is a background for new material development (industrial applications)

Thank you for your attention and many thanks for cooperation & stimulating discussions with:

- I.Kamenskikh, D.Spasky, V.Mikhailin, R.Kirkin, A.Sherbinin and other person from MSU, Moscow
- A. Belsky, C. Dujardin and the team from ILM UCBL, Lyon
- Team from ISMA, Kharkov and SUCCESS project members
- R. Williams and the team from WFU, Winston-Salem
- W. Moses, G.Bizarry and colleagues from LBNL
- V.Nagirny, A.Lushchik, M.Kirm Tartu University
- S. Payne, LLNL
- S.Keresit, F.Gao, PNL
- P.Lecoq and CCC collaboration, CERN
- P.Dorenbos, I.Khodyuk, Delft TU
- J. Singh, Darwin Univesity
- M.Korzhek, Minsk
- P.Martin, H.Bachau, CELIA, Bordeaux
- G.Zimmerer, Hamburg University
- A.Voloshinovsky, Lviv University
- and many others....



**Thank you for your attention
and cooperation!**

Probability of geminate e-h recombination

$$p(E_{e0}) = \int_0^{\infty} \left(1 - \exp\left(-\frac{R_{ons}}{r}\right) \right) f(r, l_e(E_{e0})) dr$$

where R_{ons} is Onsager radius

$$\frac{e^2}{4\pi\epsilon_0\epsilon_{st}R_{ons}} = k_B T \quad \longrightarrow \quad R_{ons} = \frac{e^2}{4\pi\epsilon_0\epsilon_{st}k_B T}$$

and $f(r)$ is spatial distribution function

$$f(r, l_e(E_{e0})) = \frac{3\sqrt{6}r^2}{\sqrt{\pi}l_e^3(E_{e0})} \exp\left(-\frac{3r^2}{2l_e^2(E_{e0})}\right)$$

$l_e(E_{e0})$ is the thermalization length

Recombination in the case of high excitation density

- A model of electron relaxation and capturing in the case of high concentration of charged centers, when Onsager radius R_{Ons} is about mean electron-hole distance $\langle r_{ec} \rangle$ (beyond the applicability of V.N. Abakumov, V.I. Perel', and I.N. Yassievich, Binding of electrons and holes into excitons, Soviet Physics – JETP, 51 (3), 626, 1980)

$$R_{Ons} = \frac{e^2}{\epsilon k_B T}$$

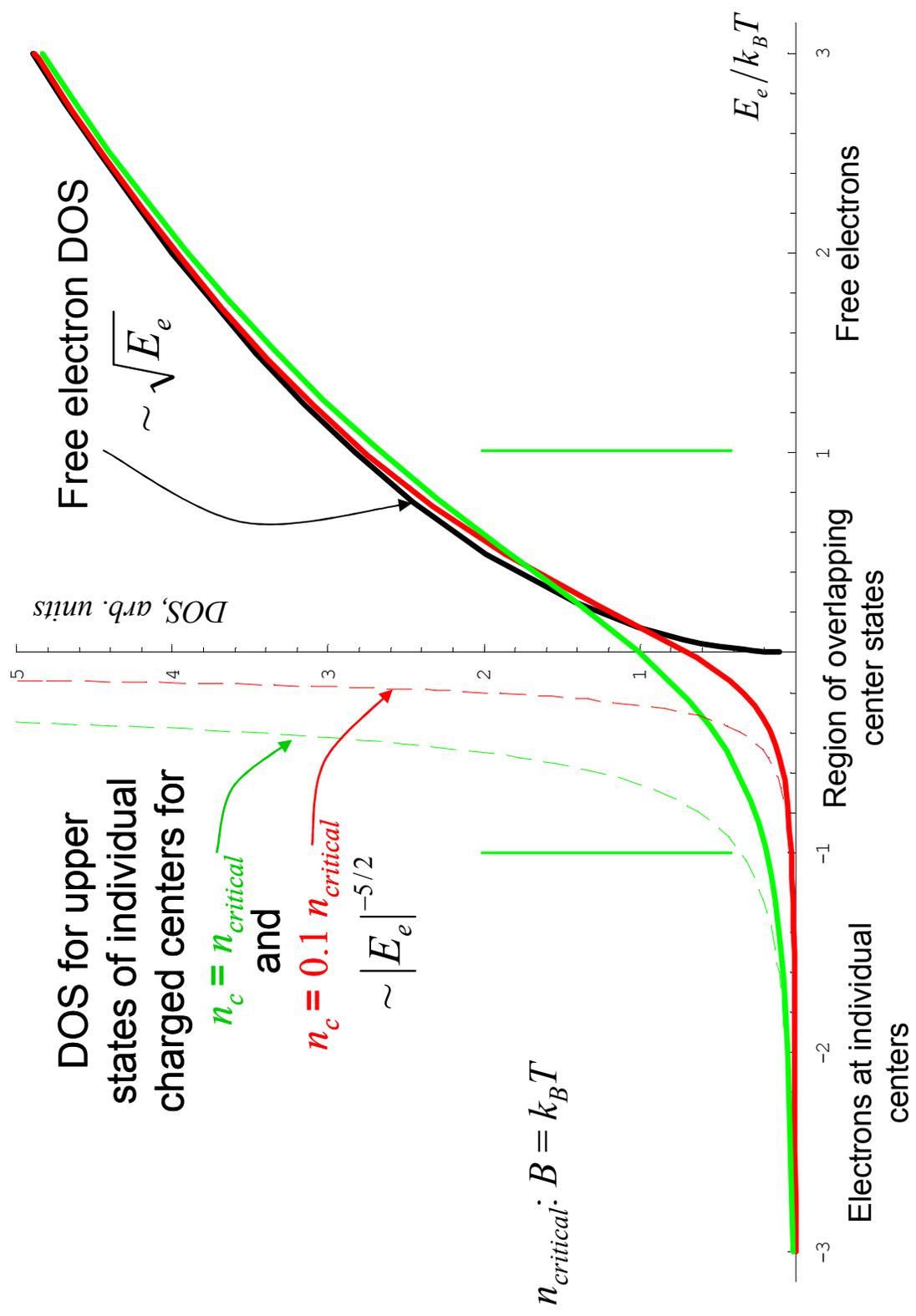
$$\langle r_{ec} \rangle \approx n_c^{-1/3}$$

- The model can be applied for rare-gas solids where only acoustic phonons exist and therefore electron relaxation is slow enough (nanosecond region) (M. Kirm, V. Kisand, E.Sombrowsky, B. Steeg, S. Vielhauer, and G. Zimmerer, Low Temperature Physics)

$$B = \pi^{2/3} n_c^{1/3} e^2 / \epsilon$$

$$\beta = \frac{B}{k_B T}$$

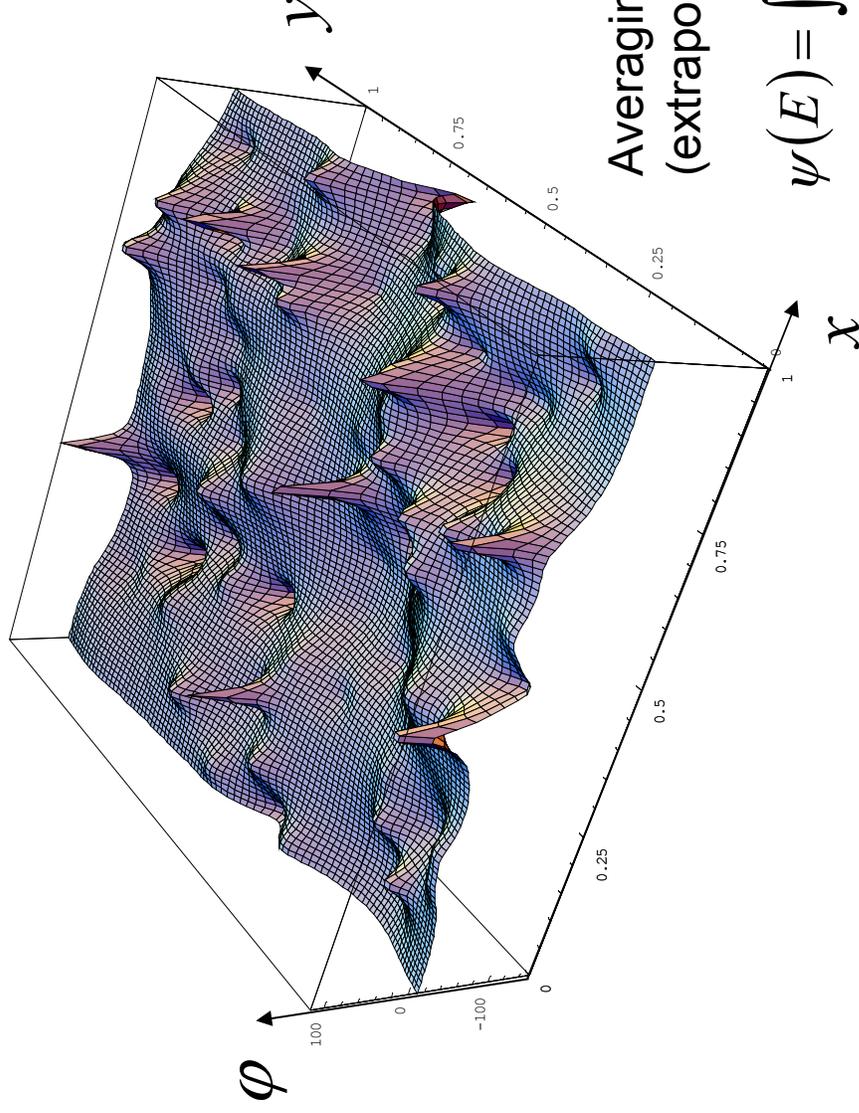
Electron density of states for crystal with high concentration of charge carriers



Random Coulomb potential example

Distribution of Coulomb potential

$$W(\varphi) \approx (2/\pi)(\varphi^2 + B^2)^{-2}$$



Averaging of free electron functions
(extrapolation to negative energy region)

$$\psi(E) = \int \psi_{free}(E - \varphi) \theta(E - \varphi) W(\varphi) d\varphi$$

Equations of electron energy diffusion for high center concentration

- Energy diffusion equation

$$\frac{\partial f(E, t)}{\partial t} = \frac{\partial}{\partial E} \left\{ D^E(E) g(E) e^{-E/k_B T} \frac{\partial}{\partial E} \left[\frac{f(E, t)}{g(E)} e^{E/k_B T} \right] \right\}$$

- Electron density of states

$$\tilde{g}(\tilde{E}) = \frac{(\tilde{E} + \sqrt{1 + \tilde{E}^2})^{3/2}}{\sqrt{1 + \tilde{E}^2}}$$

- Energy diffusion coefficient

$$g(\tilde{E}) D(\tilde{E}) = (1 + \tilde{E}^2)^{1/4} (\tilde{E} + \sqrt{1 + \tilde{E}^2})^{3/2}$$

$$\tilde{E} = E / B \quad B = \pi^{2/3} n_c^{1/3} e^2 / \varepsilon$$

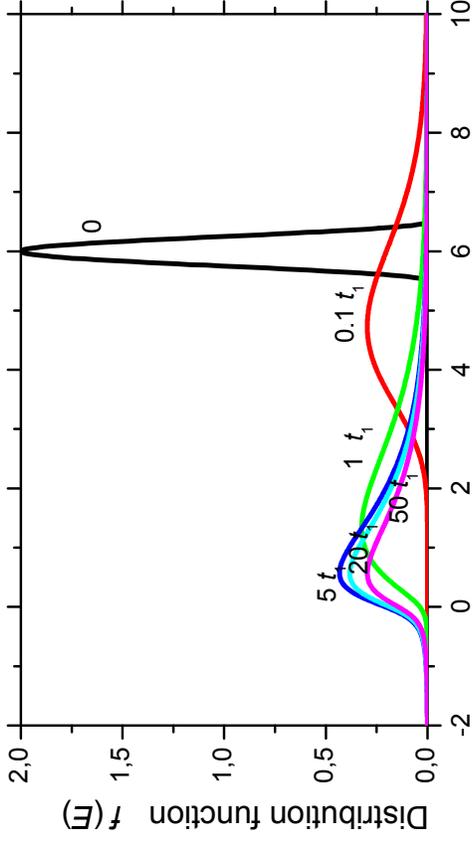
Evolution of electron energy distribution function

$$T = 5.5 \text{ K}$$

$$t_1 = 5.4 \text{ ns}$$

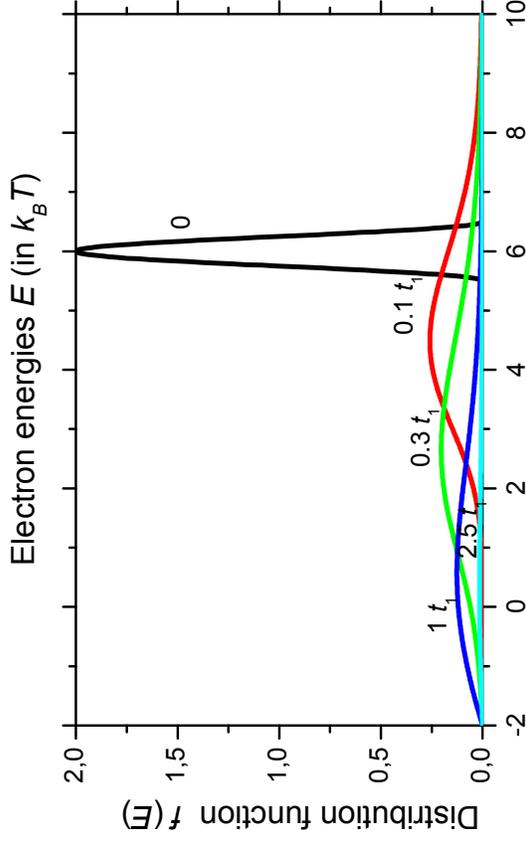
$$n_c = 10^{15} \text{ m}^{-3} \quad (\beta = 0.346)$$

Boltzman distribution is achieved at $t \sim 2t_1$

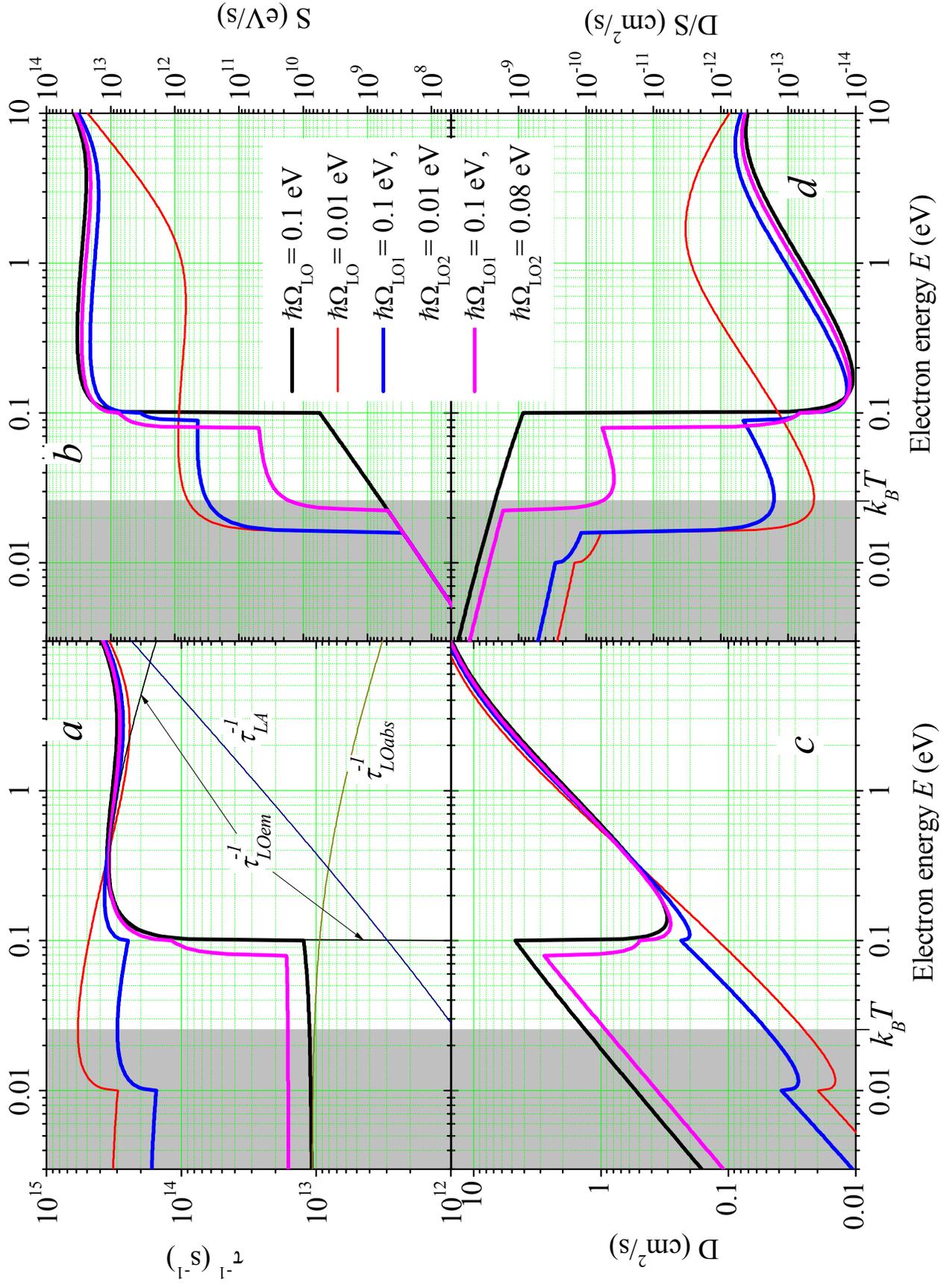


$$n_c = 10^{18} \text{ m}^{-3} \quad (\beta = 3.46)$$

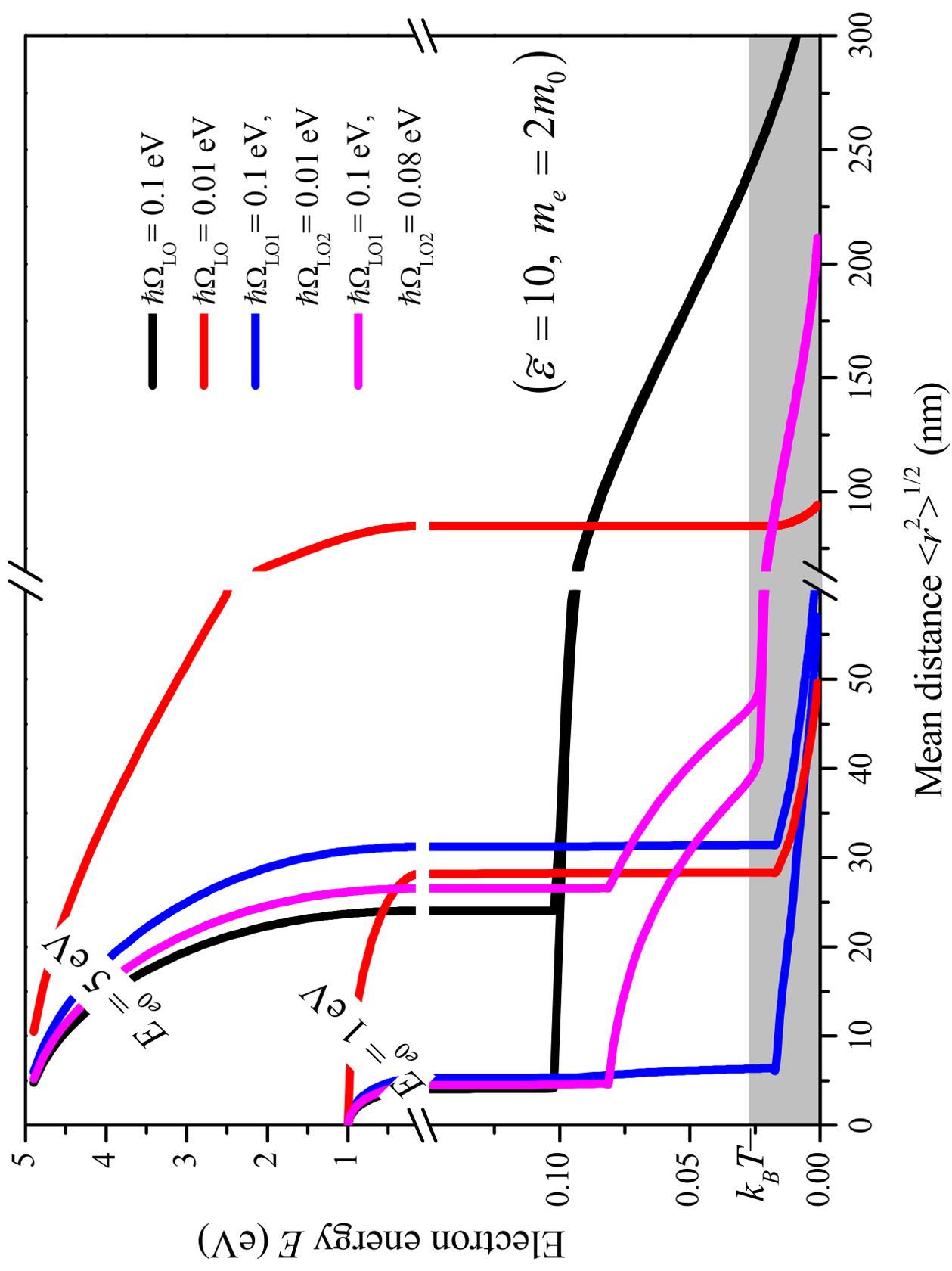
Boltzman distribution is never achieved



Estimation of relaxation parameters $(\tilde{\varepsilon} = 10, m_e = 2m_0)$



Estimation of mean thermalization length vs relaxing energy



Spatial and temporal characteristics of processes in scintillators

Spatial characteristics:

- Overall track length
- Distance between elementary e-e scattering events – e-e mfp
- **Thermalization distances**
- Recombination radius - Onsager
- Interaction (quenching) distance R_{dd}
- Activator to activator distances – concentration^{-1/3}
- Geometry dimensions – nano?

Distributed over wide range, $mfp(E)$

Distributed over wide range, $l(E_{kin})$

Time characteristics:

- Cascade time
- **Thermalization time**
- Migration kinetics before recombination
- Emission center radiation kinetics

Distributed over wide range

Elastic scattering on impurities and carriers

$$\frac{1}{\tau} = \nu \sigma N = \sqrt{\frac{2E}{m^*}} \sigma N$$

Charged impurities/carriers: Conwell & Weisskopf (Phys. Rev. 77, 388-390, 1950)

$$\sigma_c^{CW} = 2\pi \left(\frac{Ze^2}{4\pi\epsilon_0\epsilon_{st}2E} \right)^2 \ln \left(1 + 4 \left(\frac{E}{E_m} \right)^2 \right), \quad E_m = \frac{Ze^2}{4\pi\epsilon_0\epsilon_{st}m}, \quad r_m = \frac{1}{2} n_c^{-1/3}$$

$$\sigma_c^{CW} = \frac{1}{2} \pi R_{Oms}^2 \left(\frac{k_B T}{E} \right)^2 \ln \left(1 + \left(\frac{E}{k_B T x_m} \right)^2 \right), \quad x_m = R_{Oms} n_c^{1/3}$$

$$\frac{1}{\tau} = \sqrt{\frac{2k_B T}{m^*}} \frac{1}{2} \pi R_{Oms}^2 \left(\frac{k_B T}{E} \right)^{3/2} \ln \left(1 + \left(\frac{E}{k_B T x_m} \right)^2 \right) n_c = 1.5 \times 10^{-5} \left(\frac{k_B T}{E} \right)^{3/2} \ln \left(1 + \left(\frac{E}{k_B T x_m} \right)^2 \right) n_c [\text{cm}^{-3}] \frac{1}{s}$$

Neutral impurities

$$\sigma \approx 20 \frac{ka^*}{k^2}, \quad k = \frac{1}{\hbar} \sqrt{2m^* E}, \quad a^* - \text{impurity Bohr radius}$$

$$\sigma \approx \frac{20a^*\hbar}{\sqrt{2m^* E}}, \quad \frac{1}{\tau} = \frac{20a^*\hbar}{m^*} n = 1.2 \times 10^{-7} n [\text{cm}^{-3}] \frac{1}{s} = 1.2 \times 10^{13} n [\text{mol.}\%] \frac{1}{s} \quad (a^* = 1\text{nm}, m^* = m_e)$$

Processes before recombination

- Electrons and holes after cascade of inelastic scatterings are distributed in energy (with kinetic energies below E_g , i.e. the threshold of inelastic e-e scattering) and in space (with characteristic distances equal to e-e mean free paths)
- Electrons and holes are produced as e-h pairs; each generate e and h are created in the same physical point and then go away from the birthplace during thermalization (**thermalization distance**)
- Probability and kinetics of recombination depends on spatial and temporal characteristics (**diffusion of thermalized excitations with recombination**)